



UNIVERSITÀ
POLITECNICA
DELLE MARCHE

ENGINEERING FACULTY

MASTER DEGREE IN BIOMEDICAL ENGINEERING

**Design of 3D printed custom-made
orthopedic insoles**

ADVISOR:

PROF. MARCO MANDOLINI

DEGREE THESIS OF:

SIMONE RAFFAELLI

I. Summary

I. Summary	i
II. List of figure	iii
III. List of tables	v
1 Introduction	1
2 State of the art	4
2.1 Plantar pressure and plantar shear as causes of ulcers in diabetic patient	4
2.2 Foot stress measurement techniques	8
2.3 Footwear and insoles to relief plantar stress	10
2.3.1 Custom-Made insole	12
2.3.2 Insole design procedure	15
2.3.3 Material	18
2.4 Additive manufacturing applied to footwear industry	19
2.4.1 Technical background	19
2.4.2 Technologies	21
2.4.3 Additive manufacturing production of anatomical insoles	23
3 Method	25
3.1 Lattice structures and unit cells	26
3.1.1 Classification	26
3.1.2 Property	27
3.1.3 Manufacturing methods	27
3.1.4 Lattice structures design	28
3.2 Characterization of unit cells	32
3.3 Material (TPU)	36
3.4 Boundary condition	38
3.5 Insole	39
4 Case study	41
4.1 Software: nTopology	41
4.2 Cells characterization	43
4.2.1 Creation of Lattice Body	43
4.2.2 Finite element model generation	45
4.2.3 Static analysis	47
4.3 Insole modelling	49

4.3.1	Cad model	49
4.3.2	Baropodometric maps	50
4.3.3	Insole filling with lattice	51
5	Result & Discussion	58
6	Conclusion	67
7	Bibliography	70
8	Appendix	75

II. List of figure

Figure 2.1: Diabetic foot Ulcer.	5
Figure 2.2: Plantar pressure and shear stress rappresentation.	8
Figure 2.3: Platform-based sensor systems to measure plantar pressure.	9
Figure 2.4: In-shoe foot plantar system.....	10
Figure 2.5: Anatomical Insole.	11
Figure 2.6: The Glidesoft insole: a particular insole to reduce shear force.	14
Figure 2.7: Schematic diagram of the Selective Laser Sintreering system.	22
Figure 2.8: Schematic diagram of the Fused Deposition Modeling system.....	23
Figure 3.1:Three types of lattice structures, (a) Random lattice structures. (B) periodic lattice structures. (C) Conformal lattice structures.	26
Figure 3.2: Some of the most common cell unit topologies.....	29
Figure 3.3: Several TPMS unit cells.	30
Figure 3.4: Representation of texting mapping method proposed by Chen, to generate a customized lattice structure.	31
Figure 3.5: Example of a specimen build with the FCC unit cell.....	33
Figure 3.6 Different views of the Diamond unit cell.	34
Figure 3.7: Samples characterized by Octet lattice topology with different sizes and same dimensions of struct diameter of 1,5mm. A) Cell size of 15 mm. B) Cell size of 9mm.....	35
Figure 3.8: Image of an insole manufactured with TPU material.....	36
Figure 3.9 Boundary condition applied to the samples to perform the simulation.	38
Figure 4.1: nTopology logo.	41
Figure 4.2: Creation of rectangular box that delimit the design space.....	43
Figure 4.3: Box that define the specimen dimension.	44
Figure 4.4: Creation of rectangular cell map.	44
Figure 4.5: Cell map realized with cell dimension of 10mm.....	44
Figure 4.6: Lattice body creation inside the cell map, specifying the lattice topology.	45
Figure 4.7: Sample with FCC unit cell and struct diameter of 1mm.	45
Figure 4.8 Creation of the Mesh to define the finite element model for the simulation.....	46
Figure 4.9: Mesh of the specimen.	46

Figure 4.10: Set the Material Properties for the specimen.....	47
Figure 4.11: Define Boundary condition to perform the static analysis.....	48
Figure 4.12: Application of Boundary conditions.....	48
Figure 4.13: Cad model of the insole.....	49
Figure 4.14 : Upper and lower layer of the insole.....	50
Figure 4.15: Pressure Map.....	51
Figure 4.16: Shear Map.....	51
Figure 4.17: Cell Map for the insole model.....	52
Figure 4.18 Ramp block for modify cells size.....	53
Figure 4.19 Map deformation based on the pressure level.....	54
Figure 4.20 A) Original cell map. B) Warped cell map.....	54
Figure 4.21 : Insole lattice realized with variable cells size.....	55
Figure 4.22: Procedure to modify the struct diameter.....	55
Figure 4.23: Lattice map with variable struct diameter in function of the pressure map.....	56
Figure 4.24 : Command to create lattice body inside the insole.....	56
Figure 4.25: Lattice insole with variable structs dimension.....	57
Figure 4.26: Final insole models created with the two ways. A) Insole built by using the octet topology, deforming the cells from 9 to 18 mm and keeping the diameter of the struct constant to 1,5 mm. B) Insole constructed using octet topology, cell size fixed at 12 mm and struct diameter ranging from 1 to 2 mm.....	57
Figure 5.1 Static analysis of a sample build with FCC unit cell, subjected to the maximum intensity of loading. Deformation of the specimen is displayed.....	58
Figure 5.2: Results of the analysis. A) Horizontal displacement. B) Vertical displacement. C) Von mises stress.....	59
Figure 5.3: Stress strain curve for three different specimens.....	65
Figure 5.4: Printed specimens with FCC configuration.....	66
Figure 5.5: Printed specimens with Fluorite configuration.....	66
Figure 5.6: Printed specimens with Octet configuration.....	66

III. List of tables

Table 3.1: Selected topologies for the lattice structure.....32

Table 3.2 Samples realized for each unit cell topology.....34

Table 3.3 Material properties of the TPU powder for SLS printing37

Table 3.4: Different intensity of the loads simulated with the static analysis.39

Table 5.1: Static analysis results for cell topology at 6mm cell size and 1,5 struct diameter.....59

Table 5.2 : Comparison static analysis results for cell at different density. Unit cell of 5mm with struct size of 1 and 1,5mm.61

Table 5.3: Printed specimens.62

Table 5.4: Static analysis results of the printed samples.....63

Table 5.5: Results of the analysis at different intensity of loads.64

Table 8.1: Results of the numerical analysis with the samples: first part.75

Table 8.2: Results of the numerical analysis with the samples: second part.77

1 Introduction

Diabetic foot ulceration is the most common complication of diabetes mellitus; it is expected that 19%-34% of people with diabetes will develop a foot ulcer at some point of life. The cause of diabetic foot ulceration is multifactorial; however, peripheral neuropathy, associated with external forces are recognized as the principal causative factor that can lead to rise of foot ulcer. Repeated normal stresses (pressure and shear) during walking play an important role for the skin breakdown. Studies have shown that reducing the plantar stresses by offloading, in diabetic patients, helps in preventing and treatment diabetic foot[1].

To prevent ulceration and re-ulceration, the custom-made insole (CMI) is commonly prescribed to redistribute the peak plantar pressure under bony prominences in a diabetic foot with neuropathy. It has been proved that custom made insoles, compared to ordinary flat insoles can effectively decrease the peak plantar contact pressure and increase the contact area, thereby reducing the probability of foot ulcers in diabetic patient.

Traditionally, the production of anatomical insoles for a given user was carried out by subtractive manufacturing (SM) techniques, in which objects are constructed by successively cutting material away from a solid block of material using a CNC machine. With regard to the production of anatomical insoles, subtractive manufacturing poses certain drawbacks. Latest advances in additive manufacturing (AM) techniques and in particular, the popularization of 3D printing by fused deposition modelling (FDM) and selective laser sintering (SLS), have opened new ways for the production of anatomical insoles. These technologies allow additional functionalities to be added, as for instance the use of materials with antimicrobial properties, or, at a structural level, zonal control in 3D design to increase cushioning capacity. Several studies have demonstrated the potentiality of AM for design and manufacture footwear and orthoses.

The lattice structure is a type of architecture that has struts and nodes in a three-dimensional (3D) space. Lattice structures are a kind of porous material formed by repeated arrangement of unit cells, with different topological geometries. Due to their excellent elastic and energy absorbing properties, they are particularly suitable for making shoe soles and insole designs.

The material distribution in the lattice structures orthoses can be trimmed to reduce and adequately distribute plantar pressure and can also be customized by adjusting the relative density.

FE finite element method to model the foot-insole structure and to analyze the effects of different insole combinations, it proved to be a promising means for predicting the stress distributions in the foot-insole interface if the complex geometry and material conditions of the foot and insole are properly considered.

This study proposes a method to design a custom-made insole to optimize and relief stresses distribution. The lattice structures are used to create an insole with variable material properties for reducing both pressure and shear. Different topologies, such as, Body Centered Cubic (BCC), Simple Cubic, Diamond, Face Centered Cubic(FCC), Octet, Fluorite are used to create lattice material. For a better study of the following unit cells, several samples are constructed, characterized by the repetition of the unit cell selected for the entire lattice that made up the specimen. The material selected for design the insole and the specimens is the Thermoplastic polyurethane TPU and its material properties are employed in the modeling work. Finite element analysis (by using the nTopology CAD Software) is conducted to study the distribution of stresses in the different samples, by applying the boundary conditions. It is found that the plantar stress is highly influenced by the lattice topology. The best topologies in terms of stress distribution, energy absorption capacity and stiffness (related to the density) are selected and used to model the insole with lattice. Then the material distribution of the insole is modified in function of the plantar pressure and plantar shear (by using the relative loading\ maps) to improve stresses distribution.

Some specimens created by using the selected unit cells are printed employing the SLS technology, to test the quality of the samples created and the material adopted and validate the printing technique. The Octet, Fluorite, FCC topologies is found to be the most suitable of all designed cells for the insole, and have the more uniform stress distribution. The Simple cubic, BCC and Diamond have high deformation and good energy absorption but due to the elevated internal stress, these structures are discarded. NTopology has demonstrated good creation and processing skills with lattice structures and an interesting method to create areas with different properties, by using the loading maps. A limitation in the design process used is that by filling the insole with a periodic lattice structure, the cells will be trim at the sides thus forgiving the mechanical properties that characterized the single cell. For what concern the specimens made with the SLS process, they have good component qualities and high detail accuracy. Therefore, also for the eventual manufacturing of the insole can be considered the SLS and an object with high precision is expected. This has proven to be a good low-cost printing technique, but it is also possible to perform an evaluation with other methods to verify printability, such as FDM.

Future studies will be able to carry out the experimental verification of the specimens printed and compare these results with those collected from the numerical analysis. Also, the FEA of the insole can be performed; the creation of a simplified three-dimensional FE model of a human foot to study the contact mechanics of the interface between the foot and the insole, and experimental mechanical test to validate the model and verify the effectiveness of the insole in redistributing pressure compared to a flat insole.

2 State of the art

2.1 Plantar pressure and plantar shear as causes of ulcers in diabetic patient

Diabetic foot ulcer is a type of ulcer, which is a major complication of diabetes mellitus and probably the main component of diabetic foot. Diabetes Mellitus or diabetes is a metabolic disorder characterized by a high blood sugar level over a prolonged period of time, due to either the pancreas not producing enough insulin, or the cells of the body not responding properly to the insulin produced[2]. It is expected that 19%-34% of people with diabetes will develop a foot ulcer at some point and precedes 84% of all diabetes-related lower-leg amputations; for this, it constitutes a serious risk for infection and amputation[3]. Prevention of foot ulceration occurrence and reoccurrence are now recognized as key strategies in reducing the concomitant burden to patients with diabetes and the healthcare system.

An ulcer is a painful sore that is slow to heal and, in some cases, reoccurs. Ulcers can appear anywhere in or on your body, from the lining in your stomach to the outer layer of your skin. There are different types of ulcers classified according to the area of the body where they are located.

The cause of diabetic foot ulceration is multifactorial. Anyone who has diabetes can develop a foot ulcer. Native Americans, African Americans, Hispanics and older men are more likely to develop ulcers. People who use insulin are at a higher risk of developing a foot ulcer, as are patients with diabetes-related kidney, eye, and heart disease. Being overweight and using alcohol and tobacco also play a role in the development of foot ulcers[4].

Patients who have diabetes for many years can develop neuropathy, a reduced or complete lack of ability to feel pain in the feet due to nerve damage caused by elevated blood glucose levels over time. Peripheral neuropathy and a history of ulceration are the strongest predictors of ulceration [5]. Systematic reviews have demonstrated that plantar pressures are significantly higher in patients with diabetic peripheral neuropathy with a history of foot ulceration compared to those with diabetic neuropathy without a history of ulceration. However, neuropathy alone may not cause plantar ulceration. Neuropathy in combination with other factors, such as poor circulation, foot deformities, peripheral arterial disease, irritation (such as friction or pressure), and trauma, as well as duration of diabetes, can lead to the formation of plantar ulcers (Figure 2.1).



Figure 2.1: Diabetic foot Ulcer.

An important risk factor associated with the development of diabetic foot ulcers, is given by the external force act on the foot. Repeated normal stress (pressure) and shear stress during walking contribute to callus formation in the plantar region . A callus is an area of thickened skin that forms as a response to repeated friction, pressure, or other irritation. Since repeated contact is required, calluses are most often found on the feet and hands, but they may occur anywhere on the skin. Callus formation may lead to the development of foot ulcers and involves hyperkeratosis caused by excessive mechanical loading [6].

The callus formation precedes ulcer formation in over 82% of patients with diabetic foot ulcers. The relative risk for ulceration in a callused area was 11.0 compared with that of an area without callus.

High incidence of foot lesions and ulceration are at the plantar region of metatarsal heads (MTHs), where plantar pressures are mostly the highest. Reducing high plantar loads or foot pressures is one mechanism by which foot ulceration may be prevented.

Peak pressure has often been associated with ulcer presence and thus frequently assessed in the literature. Peak pressure is the highest-pressure value recorded over the entire period of the stance phase, by the device used to measure the pressure, such as the sensors of the baropodometric map. A study that examined whether plantar ulcer locations matched peak pressure sites, only 38% of the ulcers developed under the peak pressure area[8]. Murray et al.[7] has reported a 57% ulcer incidence at high pressure areas; however, it was not clear whether all wounds were observed at peak pressure points. They also disclosed the relationship between callus and ulcer locations, which may be a consequence of excessive shearing. Therefore, foot pressure was labeled as a “poor” predictor of diabetic ulcer occurrences and their location.

Historically, shear stress research has been hampered by an underestimation of the importance of plantar shear and a lack of technology to quantify it, due to the technical difficulties involved in measuring. Shear sensor technology has been still far from miniaturization to the point where it could accurately map shear load distribution. The shear stress has been commonly measured as ground reaction forces typically along, with a force platform providing resultant force acting on the outsole or barefoot because of technical difficulties. This fact appears to have acted as an almost complete barrier to practical, useful research relating to friction loads[9]. However, it is important to measure the shear stress for considering the callus related factors. The shear stress of the callus formation area is rarely measured in patients with diabetes, and therefore, there are few studies on shear stress in patients with diabetes.

Studies that were intended to demonstrate that plantar shear is also responsible as a causal factor in diabetic foot ulcers[10] , recognized shear stress as a major causative factor by stating that it is shear rather than vertical load that is responsible for tissue breakdown that occurs deep to the skin. Shear stresses act tangentially in anteroposterior and mediolateral directions at the foot-ground interface, transmitting a complex stress-strain pattern to the sublayers of the plantar tissue. These stresses are applied in alternating directions and are abrasive to the plantar surface, particularly during walking. Plantar shear distribution depends on local frictional properties of the sole, gait velocity, and, most likely, the internal muscle activity.

Emerging evidence within the past decade has demonstrated the clinical significance of shear to foot ulceration. Zhang et al., concluded that the effects of shear are additive to vertical pressures causing damage to the deeper soft tissues, as well as causing superficial damage. They noted that the internal compression stress in underlying soft tissues is a resultant of both pressure and shear components, which have been shown to have equal effects in the reduction of blood flow in tissues[11].

Among plantar shear studies, some of these indicated overlapping locations for peak pressure and shear. Instead, other have shown that peak plantar pressure and shear sites may differ in diabetic neuropathic subjects [12].

In conclusion, from these studies, which have tried to associate diabetic foot ulcers with external forces, it emerges that shear stress should be used together with pressure to better predict the risk of developing diabetic foot ulcer (Figure 2.2).



Figure 2.2: Plantar pressure and shear stress representation.

2.2 Foot stress measurement techniques

The typical components of a system used to measure plantar pressures or shear include the measuring device, which consists of sensors in a platform or insole configuration; a computer for data acquisition, storage, and retrieval for analysis; and a monitor for displaying data. There are a variety of plantar pressure and plantar shear stress measurement systems but in general they can be classified into one of two types: platform systems and in-shoe systems. In designing plantar pressure measurement devices, the key requirements are spatial resolution, sampling frequency, accuracy, sensitivity, and calibration.

Platform systems are constructed from a flat, rigid array of pressure sensing elements arranged in a matrix configuration and embedded in the floor to allow normal gait. Platform systems can be used for both static and dynamic studies but are generally restricted to research laboratories and represent the method most commonly used to assess the interaction of the foot and supporting surface. Although the force platform provides valuable information regarding both the vertical and shear components of the ground reaction force, it provides little information on how the plantar surface of the foot is loaded with respect to the supporting surface. One advantage is that a platform is easy to use because it is stationary and flat but has the disadvantage that the patient requires familiarization to ensure natural gait. Furthermore, it is important for the foot to contact the center of the sensing area for an accurate reading. Limitations include, space, indoor measurement, and patient's ability to make contact with the platform[14]. Figure 2.3 show a platform-based sensor.



Figure 2.3: Platform-based sensor systems to measure plantar pressure.

In-shoe foot plantar sensors are flexible and embedded in the shoe such that measurements reflect the interface between the foot and the shoe. The system is flexible making it portable which allows a wider variety of studies with different gait tasks, footwear designs, and terrains[15]. These have placed the way to better efficiency, flexibility, mobility, and reduced cost measurement systems. To be mobile and wearable for monitoring activities of daily life, the system should be wireless with low power consumption (Figure 2.4). Wireless in-shoe foot plantar measurement systems have potential application to data transfer communication systems, miniaturized biomedical sensors and other uses. They are, therefore, highly recommended for studying orthotics and footwear design but there is the possibility of the sensor slipping. Sensors should be suitably secured to prevent slippage and ensure reliable results. A further limitation is that the spatial resolution of the data is low compared to platform systems due to fewer sensors [16].



Figure 2.4: In-shoe foot plantar system.

In addition to these measuring systems, other types of sensors are available on the market, that use technologies such as capacitive sensors, resistive sensors, piezoelectric and piezoresistive sensors. These sensors provide electrical signal output (either voltage or current) that is proportional to the measured pressure[17].

2.3 Footwear and insoles to relief plantar stress

Diabetic therapeutic footwear is one of the essential strategies for the redistribution of plantar pressure in Diabetic Foot Syndrome (DFS). Recommendations from the International Working Group on the Diabetic Foot (IWGDF) guidelines also state that there is moderate to strong evidence of wearing customized footwear during weight-bearing activities in reduction of plantar pressure[18]. In DFS, even customized insoles often prescribed to reduce mean plantar pressure by redistributing from metatarsal heads and other areas, reducing the risk of ulceration and its recurrence .

Orthopedic footwear are shoes used to correct, accommodate, or prevent a physical deformity or range of motion malfunction in a diseased or injured part of the foot. This typology of footwear is classified as medical devices. Nowadays, with the new knowledges acquired in the field of biomechanics and the use of methods assisted by computerized systems, the construction of orthopedic footwear is carried out with technical-scientific rules, which aim, to restore the functionality of the foot taking into account the static, the dynamics, the lower limb, the spine and the aesthetic part [19]. An orthopedic footwear is built from the same elements as a regular shoe, but some of these are processed in order to confer certain characteristics and design features to carry out corrective actions and give greater comfort to the foot, such as extra widths, taller upper-soles, supportive heel, a well cushioned and strong mid-sole, characterized by impact absorption properties. Among the orthopedic footwear there are the custom-made orthopedic shoe, typically recommended for the most serious or complex cases. This medical device is designed specifically to meet the patient's needs, thus are produced for specific type of patients, based on the pathology and deformity of the subject and its manufacture requires an advanced scientific technical knowledge.

In the field of footwear, the insole (Figure 2.5) is a component located between the foot and the shoe sole. Being in direct contact with the foot, the insole supports body weight. Therefore, it directly affects the biomechanics of the foot and the body, with a specific strategy for minimizing potentially harmful tissue stress on the foot's plantar region.



Figure 2.5: Anatomical Insole.

There are certain essential aspects characterizing an insole. Firstly, its morphology, in that it has to be adapted to the anatomy of the foot sole, which is characterized by three main arches. These arches shall be adequately balanced to achieve perfect support. Secondly, the density of the materials chosen for production, which directly redounds to certain properties, like flexibility, hardness, resistance, shock absorption. There are also other corrective elements, called additions, which are added on the metatarsal area of the insole in order to retain the foot in an anatomically correct position and dampen impacts while walking[20]. An anatomical insole should be intended to reduce and adequately distribute plantar pressure among support points, thus minimizing the stress these points can undergo during the execution of physical activity or while standing for long periods patients.

2.3.1 Custom-Made insole

Custom-made insoles (CMI) are a medical device that are part of the orthopedic insoles. The main feature is that these devices have a tailor-made production related to the pathology, anatomy, age, weight, other anatomical characteristics, and information of the individual patient. Hence, it is unique. The insoles are considered “customised” if specific data from the patient foot is used in the design process, typically foot shape and pressure distribution [21]. Can be prescribed for the treatment or prevention of a wide range of foot and lower limb problems with several potential aims. These are total contact insoles (TCI) ; insoles custom-molded according to the plantar geometry of the patient’s foot in order to provide accommodative support, and to redistribute and reduce high plantar pressures under the heel and the metatarsal regions. Are frequently prescribed for individuals with diabetic neuropathy to reduces the risk of plantar ulceration. Insoles provide the important interface between the foot and the shoe and, together with outsole modifications, offer the most direct approach to the reduction of potentially damaging tissue stresses on the plantar aspect of the foot.

The Medicare Therapeutic Shoe Bill recognized the importance of this intervention for the prevention of primary and secondary ulcers, thanks to the offloading and redistribution of plantar pressure. Although the design and manufacturing of insoles vary among practitioners and manufacturers, the plantar pressure offloading is generally achieved through the use of pads (e.g. metatarsal bar, metatarsal dome, heel pad), cavities, cuts out or combining layers of different materials in different plantar areas. Several studies investigated the amount of pressure reduction for different padding and insole materials commonly used in the podiatry clinic[22]. The plantar pressure offloading consists in the identification of the plantar areas with pressure peaks and the design of appropriate personalized insoles in terms of geometry and materials.

One of the main methods used to evaluate the benefits of orthopedic insoles is by comparing load distribution patterns from a CMI and some controlled conditions, such as a flat insole, worn sequentially both on the same foot and in the same shoe, from which load transfer analysis can be performed. The main off-loading techniques used for the CMIs were the removal of material under high-pressure areas and the build-up of material at other locations using the metatarsal pad and a medial longitudinal arch support integrated into the insole. Substantial “heel cups” were also a feature of the CMIs. A different offloading technique consists in the right selection and combination of materials on different areas of the insole, selecting soft materials under high-pressure areas and stiffer material at other locations[23].

Increasing the thickness and changing the mechanical properties of material under bony prominences is an effective approach to the reduction of plantar pressure, although there is a lack of systematic studies that could help predict the optimal design and placement of pressure relief features of various sizes, shapes, and material properties. The maximum thickness of material that can be used under the MTHs is limited by footwear depth because excessive depth can, depending on the shoe, put the patient at risk for dorsal ulceration.

Systematic reviews have demonstrated the efficacies of use tailor insole: Lord et al., have demonstrated that peak plantar pressure in diabetic patients during walking was reduced by using molded insoles compared to flat insoles, and using various types of insoles compared to no insoles[24]. Custom molded insoles were shown to reduce pressure during standing and walking in diabetic subjects, and to reduce dynamic peak pressure compared to flat insoles in healthy and diabetic subjects [25][26].

Few studies in the literature have deepened the aspect of the plantar shear and tried to develop a shear-reducing insoles that permit side-to-side motion in the device to reduce shear at the skin and deeper tissue level. Lawrence et al.[27] have tested a novel shear reducing insole, Glidesoft, produced using a combination of materials of the insole to form three types of multilaminar insoles. The GlideSoft insole design used the same combinations of materials such as standard insoles, and not alter the shape, surface, outline or thickness of the plate. It had two thin intermediate layers of low-friction materials, which slide upwards between them. The results showed that the GlideSoft technology has the ability to highly reduce shear in the insoles, significantly decreasing the peak shear force that would be applied to the skin surface during gait. As described, when a shear force is applied to the Glidesoft, the top pad of the insole moves relative to the bottom.

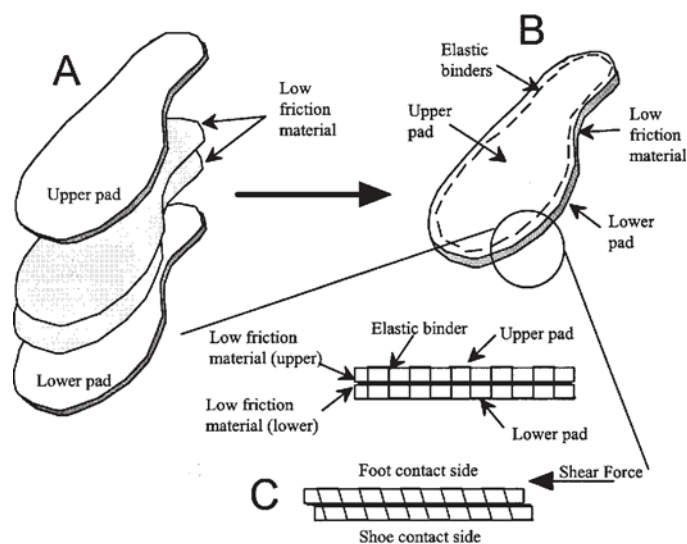


Figure 2.6: The Glidesoft insole: a particular insole to reduce shear force.

2.3.2 Insole design procedure

During the last decades the developing procedure of a custom-made insole has undergone a strong computerization starting from the foot diagnosis to the manufacturing of the orthotics. The overall procedure can be summarized in the following three different stage:

- a foot diagnosis and measurement stage, in which 3D scanners are used to obtain a high-quality virtual geometry of the foot;
- a footwear design stage, where all the elements of the insole are designed using specialized CAD tool;
- a production stage, where CNC machines or 3D printers are employed to manufacture the insoles.

The insole design phase consists both in the determination of its geometry and the set of materials to be used. The clinical practice has changed over the years. After decades where the custom-made insoles were designed just following the foot shape, different research approaches evaluated the effectiveness of custom foot orthoses based also on plantar pressure[28].

Traditional technique to produce orthotic insoles makes use of footprints in a foam box, to obtain the foot shape. Nevertheless, this method often has low precision and accuracy of the insole when assembled with the patient's foot geometry and frequently produces orthotic footwear with low comfort. Moreover, this traditional method often leads to higher costs and production time. Nowadays, thanks to 3D scanners it is possible to obtain the virtual geometry of the foot in static or dynamic mode respectively, and at the same time use the pressure platforms to obtain barefoot plantar pressure maps, with which to model the properties of the insoles[29].

With the rapidly developing computer-aided design (CAD) technology, three-dimensional (3D) design of orthotic insoles can be made for various foot contours with optimal fit and minimum production cost and design time , improving the precision and quality of the product.

The first CAD systems developed for the modeling of the insole consider only the plantar pressure and the measurements of the foot neglecting the 3D shape of the last [30]. More advanced tools consider the design of the digital insole around the digital foot (obtained using the 3D scanner) by achieving the necessary level of control over the geometry of the insole in the form of input parameters. Development of the technology has allowed to use more advanced approaches by combining CAD/CAM and CAD/CAE systems for the production of customized orthotics [29]. CAE (Computer-aided engineering) technology indicates software applications that facilitate the resolution of technological problems through numerical calculation. Among these, there is the finite element analysis (FEA), a computer simulation technique used in engineering analyzes, and even in this study, which uses the Finite Element Method (FEM).

The finite element method is used to model the foot-insole structure and to simulate the interaction between these, to predict and visualize the plantar pressure distribution of different insole combinations, in order to achieve the best geometry and materials combination. This approach has the benefit of allowing modification of different insole design and performing parametric analysis with a relatively easy procedure.

Finite element method has been employed previously in many foot-related biomechanics studies and it has been demonstrated this can be a promising means for predicting the stress distributions in the foot–insole interface if the complex geometry and material conditions of the foot and insole are properly taken into account. Several finite element models of the foot or footwear have been developed, based on certain assumptions. These assumptions include simplified geometry, limited relative joint movement, ignorance of certain ligamentous structures, and simplified material properties. Early models were based on a simplified or partial foot shape. Analyses were conducted under assumptions of linear material properties, infinitesimal deformation, and linear boundary conditions, without considering friction and slip. Recent models have improved in selected aspects by incorporating geometric, material, or boundary nonlinearity (eg, large model deformation, nonlinear material properties, slip/friction contact conditions) [31].

From the industrial point of view, several CAD-based solutions are offered on the market. They consist of software tools to design custom-made insoles and aiming at replacing the manual manufacturing processes. The most popular and advanced are paroContour System (by PAROMED)[32], Insole-Designer (by PEDCAD), IcadPAN (by INESCOP)[33]. The IcadPAN and the Insole-Designer are CAD applications that run as a plugin to the Rhinoceros CAD system. INESCOP is able to automatically generate insoles from different input data like foot measurements, the position of foot landmarks, a digital mesh of the foot or scanned insoles or lasts. It is also possible to retrieve data from databases of standard insoles or adapt the insole to a specific last.

Additionally, reverse engineering and reverse innovative design allow the rapid production of insoles with highly accurate and precise size[34].

2.3.3 Material

A wide range of materials have usually been employed for the production of shoe insoles. A customized insole is generally made at least of two/three layers of different materials. Properties such as hardness, tensile strength, rigidity, flexibility and permeability directly depend on the constituent material and have been the object of some studies. One of the most commonly employed materials over recent years is ethylene-vinyl acetate or EVA, which is a thermoset polymer supplied in sheet form in different thicknesses and sizes. EVA foam is mostly used in orthotic shoe insoles because it helps realize lightweight footwear with high comfort, resiliency, and durability[35]. It is a copolymer plastic of ethylene and vinyl acetate, it is resistant to fungus and bacteria, hypoallergic and non-toxic. For these features, orthosis in EVA foam is widely used in the treatment of foot pain ulcers, which are commonly experienced by diabetic patients.

A usual solution for the production of anatomical insoles is milling EVA blocks with different density areas using a three-axis CNC machine. The highest density area is used to produce the rear part of the insole, as it is characterized by higher hardness and provides more stability to the heel area. The least hard area is used to mill the forepart, since the metatarsal area calls for higher impact absorption efficiency .

As can be observed, this solution, even though it is more suitable for production using a single material, is little flexible and very limited. The possibility of functionalizing anatomical insoles by providing them with internal structures that locally modify shock absorption properties could meet user's needs in terms of comfort, pressure distribution correction and impact absorption in a more extensive and flexible way than how it has been done till present. However, this is not possible using traditional subtractive manufacturing techniques.

Another common material ,that is used to realize insole is the Poron (Rogers Corporation, Connecticut, U.S.A) , an open-cell polyurethane foam[36].

2.4 Additive manufacturing applied to footwear industry

2.4.1 *Technical background*

Originally, the production of anatomical insoles for a given user was carried out by subtractive manufacturing (SM) techniques. This is a process by which objects are constructed by successively cutting material away from a solid block of material using a computer numerical control (CNC) machine. With regard to the production of anatomical insoles, subtractive manufacturing poses certain drawbacks [37]. First of all, material waste upon cutting material away from the original block. Secondly, lack of flexibility to alternate materials in different areas according to the user's needs, since the material to be used is pre-determined by the original block. In addition, it is impossible to gain access to the inside of the insole. Nevertheless, the recent advances in additive manufacturing allow the limitations inherent to SM to be overcome.

Additive manufacturing (AM) is a process by which a three-dimensional object is built up by superimposing material layers using different manufacturing techniques.

The physical object is obtained through a process consisting in depositing successive layers of material of a finite thickness from bottom to top.

The AM technology has witnessed substantial improvements in recent years, brings about new possibilities when compared with traditional systems, thus avoiding many constraints. The unique capabilities of AM [38] include:

- Shape complexity: it is possible to build virtually any shape avoiding the approximations imposed by subtractive or machining methods ;
- Material complexity: it is possible to use material combinations to provide the product with new properties;
- Hierarchical complexity: multi-scale hierarchical structures can be designed and fabricated from the microstructure (size in the millimeter range) to macrostructure;

- Functional complexity: different geometries can be embedded in an object in such a way that the resulting product features new or different functionalities. These benefits can help AM notably increase industrial competitiveness in that it ensures quick responsiveness to changing market needs and growing consumer demands for product customization .

Initially it was a technology designed primarily for rapid prototyping. Subsequently, the expansion of the range of materials used by this technology, combined with the design flexibility, has allowed a diffusion of AM in various fields, such as medical for the realization of prostheses and implants, until to the realization of organs, blood vessels; energetic, aerospace, to produce parts for propulsion systems, turbine parts, combustion chambers; automotive, for the transmission and structural parts, discharge valves and for consumer products.

Compared to the traditional subtractive manufacturing technologies, it not only reduces the material used, but it also reduces the difficulty in fabricating complex geometries. The broad design freedom permitted by AM leads to more and more innovative and efficient products in industries such as aerospace, biology, and healthcare.

Process planning of AM is not as time-consuming as traditional manufacturing, which is suitable for mass customization (Paoletti, 2017).

It is mentioned that AM enables new opportunities for customization, through significant improvements in product performance, multifunctionality, and lower overall manufacturing costs[39].

AM technologies involve the use of various types of materials, two of which are of great interest in the industrial engineering sector:

- Metals: they allow to obtain very high mechanical performances, but they require more complicated and expensive technologies;
- Polymers: thermoplastic resins that allow to reduce costs both for the purchase of the material and for the printing technology.

Among the polymers only thermoplastics can be used for additive manufacturing. The main polymeric materials are PLA, ABS, nylon, which have excellent mechanical properties.

2.4.2 Technologies

There are seven different additive manufacturing technologies that make use of different production processes. Each technology is more specific, suitable for a particular type of material and for a certain field of application. These are:

- Powder Bed Fusion
- Material extrusion
- Binder Jetting
- Directed Energy Deposition
- Material Jetting
- Photopolymerization
- Sheet Lamination

Powder Bed Fusion (PBF) technologies produce a solid part using a thermal source that induces fusion (sintering or melting) between the particles of a plastic or metal powder one layer at a time. The main variations in PBF technologies come from the differing energy sources (for example lasers or electron beams) and the powders used in the process (plastics or metals). Selective Laser Sintering (SLS) is part of the PBF technologies and produces solid plastic parts using a laser to sinter thin layers of powdered material. The process begins by spreading an initial layer of powder over the build platform. The cross-section of the part is scanned and sintered by the laser, solidifying it [40]. The build platform then drops down one layer thickness, and a new layer of powder is applied. The process repeats until a solid part is produced (Figure 2.7). Both Selective Laser Melting (SLM) and Direct Metal Laser Sintering (DMLS) produce parts via the similar method to SLS. The main difference is that SLM and DMLS are used in the production of metal parts.

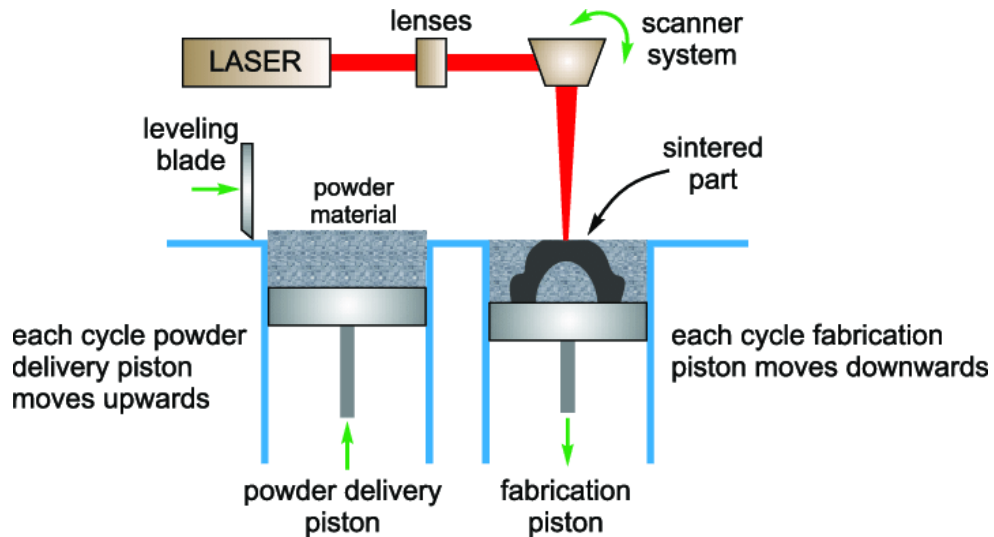


Figure 2.7: Schematic diagram of the Selective Laser Sintering system.

Electron Beam Melting (EBM) EBM uses a high energy beam rather than a laser to induce fusion between the particles of a metal powder. Polymer-based PBF technologies offer a lot of design freedom, as there is no need for support, allowing the fabrication of complex geometries.

Material extrusion technologies extrude a material through a nozzle and onto a build plate. The nozzle follows a predetermined path building layer-by-layer. Fused Deposition Modeling (FDM) is a common material extrusion process and the most widely used 3D printing technology. FDM (Figure 2.8) builds parts using strings of solid thermoplastic material, which comes a filament form. The filament is pushed through a heated nozzle where it is melted. The printer continuously moves the nozzle around, laying down melted material at precise locations following a predetermined path. When the material cools it solidifies, building the part layer-by-layer. Material extrusion is a quick and cost-effective way of producing plastic prototypes. Industrial FDM systems can also produce functional prototypes from engineering materials. FDM has some dimensional accuracy limitations and is very anisotropic.

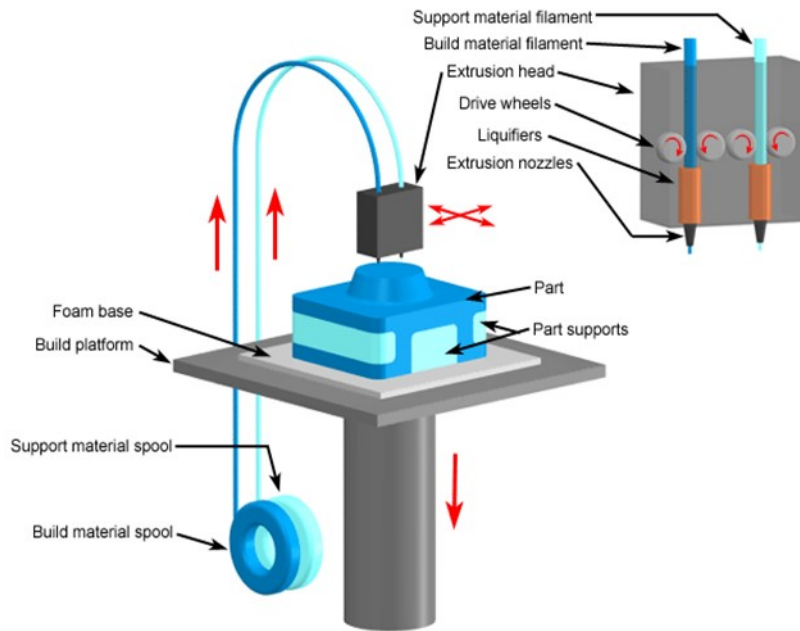


Figure 2.8: Schematic diagram of the Fused Deposition Modeling system.

2.4.3 Additive manufacturing production of anatomical insoles

AM together with three-dimensional (3-D) foot scanning are promising in terms of footwear personalization for the masses. AM allows geometric freedom and has a tool-less capability, which allows the production of personalized components directly from computer models at no extra cost. The potential of combining AM with foot scanning and CAD systems is evidenced by the growing number of papers reporting their use to produce shoe insoles[42] and orthotics.

AM has been used in the field of footwear to produce shoes, shoe soles, and insoles [43]. Its layer-by-layer strategy permits the manufacture of complex, high-performance monolithic designs with varying performance areas within a single part. Therefore, shoe soles with different stiffness zones can be easily fabricated by AM.

Davia-Aracil et al. reviewed certain CAD methodologies for the design and manufacture of insoles by means of additive manufacturing techniques. Different three-dimensional patterns are used in the heel area to incorporate new functionalities. It is concluded that the footwear industry can benefit from the advantages of AM. It is also proved that AM is cost-effective and feasible on an industrial level [38].

Common additive manufacturing technologies, used to manufacture footwear and insoles are the FDM and SLS, as shown by different reviews presented in literature.

In [44] the FDM 3D printing technique is used. One of the main advantages of FDM 3D printing is that it allows thermoplastic polymers to be used, such as polylactic acid (PLA) or acrylonitrile butadiene styrene (ABS) .

The paper [45] propose a design method using lattice structures for AM to fabricate shoe soles is. Different types of unit cell lattice structures are used to infill the design space. The fused deposition modeling (FDM) process is used to fabricate lattice shoe soles. The mechanical performance of each type of lattice shoe sole is investigated both experimentally and numerically, and results demonstrate that the different unit cells have the capacity to reduce stress distribution and produce a high energy absorption.

Due to the porous characteristic of lattice structures, it presents a new class of energy absorption materials that offer flexibility in tailoring the response to impulse loads compared to conventional materials. In this study the lattice structures technology will be investigated to try to build a custom-made insole to relief plantar stress.

3 Method

The purpose of this study is to develop a method for designing and modeling a custom-made insole, which can relieve plantar stresses. To achieve this goal, the technology that uses lattice structures in the field of additive manufacturing has been used. Lattice structures are a kind of porous material formed by repeated arrangement of unit cells, with different topological geometries (set of beam elements or supporting struts connected to nodes). The properties of lattice structures are directly related to the geometric size, shape, structure, and spatial arrangement of unit cells. Since lattice structures are used to create lightweight components by reducing the amount of material and due to their excellent elastic and energy absorbing properties, they are particularly suitable for making shoe soles and insole designs.

To simplify the process of identifying the best unit cells topologies, the overall analysis is divided into two main parts:

- Characterize the unit cells to identify the lattice structures topologies with the most suitable properties for making the insole. To do this, different specimens were made with the different unit cells and compared using Finite Element Analysis.
- Design the custom-made insole to relieve plantar stress.

From the results of the FEA, the specimens containing the unit cells that had the best properties to build the insole were selected and some of them were subjected to the printing process using SLS technology.

3.1 Lattice structures and unit cells

Lattice structures are topologically ordered, three-dimensional open-celled structures composed of one or more repeating unit cells. These cells are defined by the dimensions and connectivity of their constituent strut elements, which are connected at specific nodes. The unit cell is defined as the smallest repeating unit having the full symmetry of the lattice structure.

3.1.1 Classification

Typically, lattice structures can be divided in three different categories: stochastic, periodic or pseudoperiodic. Stochastic lattice structures are those such that their distribution of cells and shapes is defined through a random probability distribution. The unit cells of random lattice structures are randomly distributed in the design space and have different topological structures and sizes. The second category is the periodic lattice structures. This kind of lattice structures can be regarded as the structure formed by periodic repeated arrangement of lattice cells with certain shape, topology, and size in three-dimensional Euclidean space. The third kind is pseudo periodic lattice structures (also called conformal lattice structures). In pseudo lattice structures (proposed by Wang and Rosen), each unit cell only has the same topology, but its size is different (Figure 3.1).

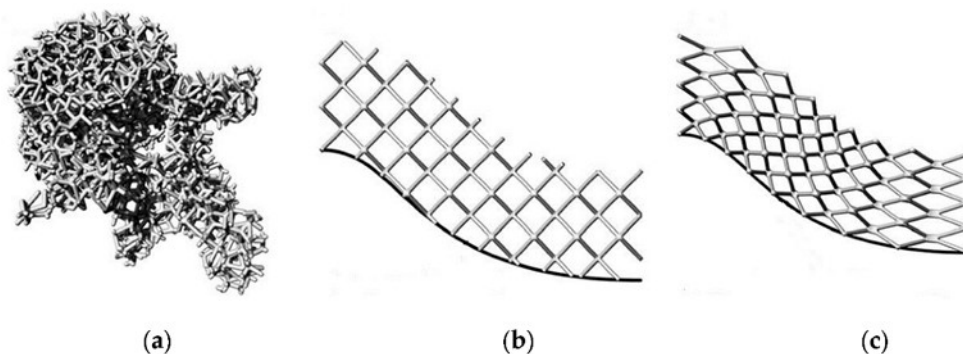


Figure 3.1: Three types of lattice structures, (a) Random lattice structures. (B) periodic lattice structures. (C) Conformal lattice structures.

In the following study the periodic lattice structure will be used for the characterization of the cells and for the filling of the insole, since that lattice distribution of material will be modified later to redistribute the stress inside the insole.

3.1.2 Property

The mechanical properties of lattice structure are the fundamental aspects for the design of lattices. Lattice structure is usually used in lightweight structure design to minimize material loss and energy consumption in the manufacturing process. Energy, material, and time of manufacturing process can be saved effectively by designing and optimizing the lattice structure. The main properties are:

- High stiffness and strength
- High energy absorption
- High damping effect
- Dissipate heat.

3.1.3 Manufacturing methods

Although it has been possible in the past, create lattice structures using traditional manufacturing methods, fabricating such complex objects has been limited due to the inability to leverage traditional manufacturing processes to create structures without requiring labor-intensive assembly processes. All traditional processes can be used to manufacture lattice structures in the mesoscale; however, they struggle to create microstructures.

A significant amount of progress in additive manufacturing fields has enabled researchers to reliably manufacture lattice structures and vary parameterized cell designs to research their behaviors. Commercial pressure and advancement in materials have pushed the technology to progress to allow for the creation of structures with greater accuracy and in higher volume, with an ever-increasing amount of additive manufacturing techniques.

Additive manufacturing (AM) technology, provides promising opportunities to fabricate structures automatically and flexibly, with complicated shapes and architectures that could not be fabricated by conventional manufacturing processes. The combination of lattice structure and additive manufacturing technology is an unprecedented breakthrough in the field of industrial design. In particular, the fabrication of lattice structures with AM technology has produced the following advantages:

- Design flexibility;
- Fabricate lattice structure with wide range of sizes;
- Many kinds of materials (rubber, metal, alloy, ceramic, fiber, etc.);
- Reduce the amount of material utilized in the manufacturing process;
- Optimize the strength of the produced object while minimizing the weight;
- Reduce the amount of energy used in the manufacturing process;
- Reduce the amount of time taken to produce an object;
- Set up program for automatic processing.

There are also some weaknesses in AM technology, i.e., when designing lattice structures with suspended geometry, support materials need to be added, which also causes certain material waste and increases post-processing.

3.1.4 Lattice structures design

A lattice is a cellular structure made of repeated unit cells to form a larger volume. There are many options for the shape and size of such lattice cells, and for the pattern in which they are repeated, and there are countless examples of lattice structures being used to reduce the amount of material, to improve its strength to-weight ratio, or to replace support material in a part[51]. Lattices can be uniform, where the same cell size is repeated in all directions of the part, or variable, where the size and spacing of the cells is different in different directions.

Most of academic work on the properties of lattice structures are based on the design of unit cell structures, the change of unit cells arrangement, and the optimization. With the application of various modeling software, it is easy to design different unit cell structures. It is possible to use CAD software to design the geometric structure of unit cells, and then analyze the performance of the unit cells by finite element or experimental methods, and finally form a uniform lattice structure according to a certain arrangement of unit cells. Many literatures have studied the design of unit cells [31]; the structures of some of these are shown in figure x. There's a vast array of cell structures, which are the repeated unit in a lattice. The list of cell structures is very long and ever-growing. For a lattice structure to be fully defined, the unit cell must be fully characterized in terms of the overall description of the structure design, generation method and intrinsic properties. Extensive studies concerning the different unit cells[], shows that there currently exists only a relatively small amount of lattice structures, of which a significant amount are slight variations of other existing cells. Each cell type should in theory possess unique capabilities that make them superior to other cells in a certain way, such as increased energy absorption or relatively high strength to weight ratios.

The most common cell structures include cubic, octet, hexagonal, diamond, face centered cubic and tetrahedron (Figure 3.2).

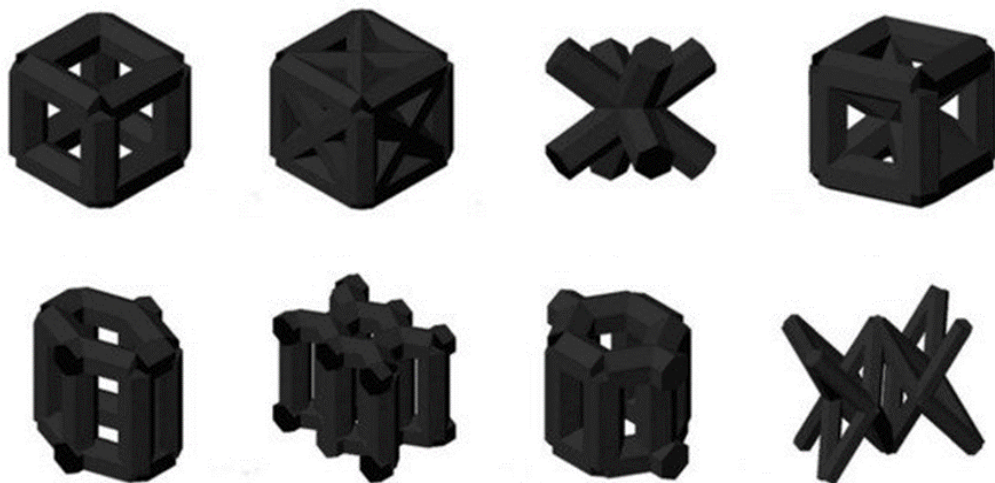


Figure 3.2: Some of the most common cell unit topologies.

There are several methods that are utilized to generate lattice structures. These are broken down into two different categories; manually generated and mathematically generated. A manually generated lattice structure is created through the utilization of beams and truss structures, with joints modified to create seamless transitions between unit cell elements. The previous unit cells are examples of manually created lattice structures.

Instead, mathematically generated lattice structures are created with algorithms and constraints, utilizing mathematically described patterns and surfaces to create a lattice structure. These structures, in contrast to manually created ones, do not need any post-processing to connect the structures as they are in most cases periodic. Triply periodic minimal surface (TPMS) is one of the mathematical methods that can successfully transform the theoretical mathematical model into the actual lattice structures. TPMS (Figure 3.3) are minimal surfaces (a surface in hyperbolic space which possesses a mean curvature or zero), which are a subset of hyperbolic surfaces. A hyperbolic surface is one created utilising hyperbolic geometry. TPMS can be generated in multiple ways including Weistreass formula evaluations, nodal approximations of the Weistreass formula, and numerical generation [50].

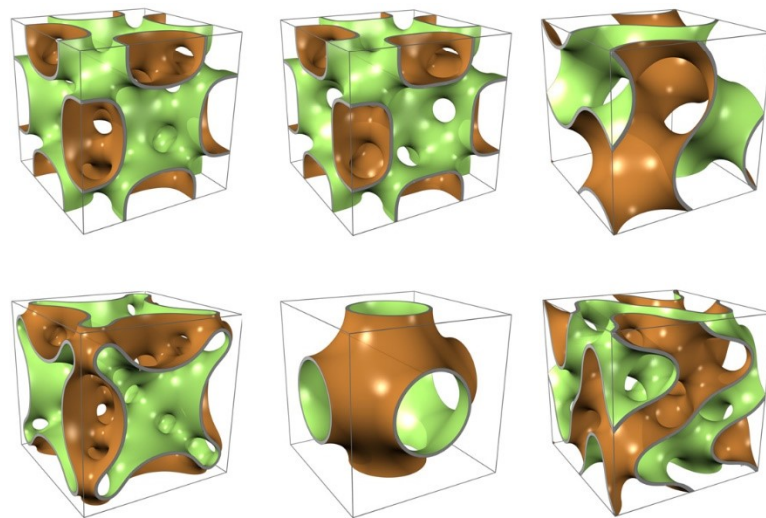


Figure 3.3: Several TPMS unit cells.

In the present study, only the manually generated lattice structures are investigated, but given the great potential of TPMS cells, further investigations can be made regarding these structures.

For the design of unit cell shape, Chen [52] proposed a 3D texture mapping method, which enabled designers to select the unit cell structure that satisfied the design requirements from cell structure library, and then the internal structure was generated and defined in the selected language file combined with the selected unit cell structure. System can automatically convert the unit cell structure file into a CAD model. Finally, all the unit cells formed a lattice structure. The basic idea of 3D texture mapping is shown in Figure 3.4. The 3D texture mapping method proposed by Chen is based on mapping a unit cell structure into a design space to generate a customized lattice structure, which makes the design of lattice structure easy.

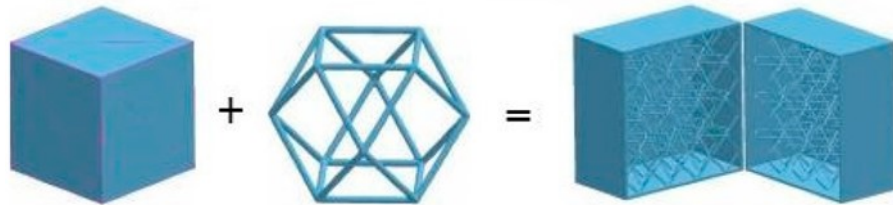


Figure 3.4: Representation of texture mapping method proposed by Chen, to generate a customized lattice structure.

There are a limited amount of commercial software tools available to aid in the design of lattice structures. These include packages such as Autodesk Within Medica (Autodesk, Inc., USA), Materialise Magics (Materialise NV), nTopology Element (nTopology, Inc., USA) and Simpleware CAD (Simpleware, Exeter, UK), as well as software plugins such as IntraLattice.

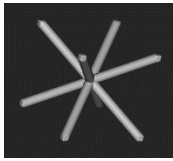
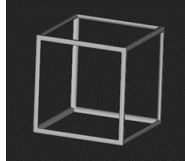
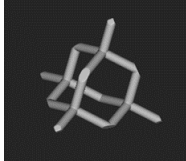
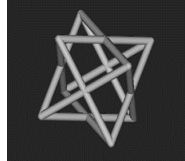
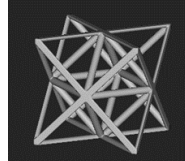
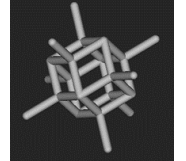
In the current study the nTopology Element software has been used to study the behavior of several lattice structure topologies.

3.2 Characterization of unit cells

To characterize the numerous unit cells ,in this study, different specimens are constructed with dimensions that approach the size of a part of the insole, such as the heel area, or the individual metatarsal heads, where the highest-pressure levels are detected.

In In this examination, six types between the most common cell topologies, as shown in Table 3.1, are investigated. These are commonly identified in the world of the lattice unit cells, with the names of Body Centered Cubic (BCC), Simple Cubic, Diamond, Face Centered Cubic(FCC), Octet, Fluorite .

Table 3.1: Selected topologies for the lattice structure.

BCC	Simple Cubic	Diamond	FCC	Octet	Fluorite
					

The first three cells are commonly used and have been analyzed by several studies in the literature, as well as in the previous article [44], where this type of cells is used to fill the inside of a midsole.

The other three topologies have not been previously analyzed in the field of footwear but have good mechanical properties, and a denser structure than the previous ones, consequently they will have a more rigid behavior.

The specimens consist of an internal volume, which represents the space intended for the lattice structure, and of two plates, one lower and one upper that correspond to the surfaces where the boundary conditions are applied. The samples are characterized by the repetition of the unit cell selected for the entire cellular map that constitutes the lattice.

These are rectangular parallelepipeds of dimensions: width and length about 30mm and height about 10mm, depending on the size of the cell that has been chosen. The plates are 1mm thick and 1mm wider than the rectangular volume (design space) intended for the lattice structure (Figure 3.5)

Each specimen is built considering the following parameters(input variable):

- Dimensions of the samples
- Unit cell topology
- Cells size and struts diameter
- Material characteristic

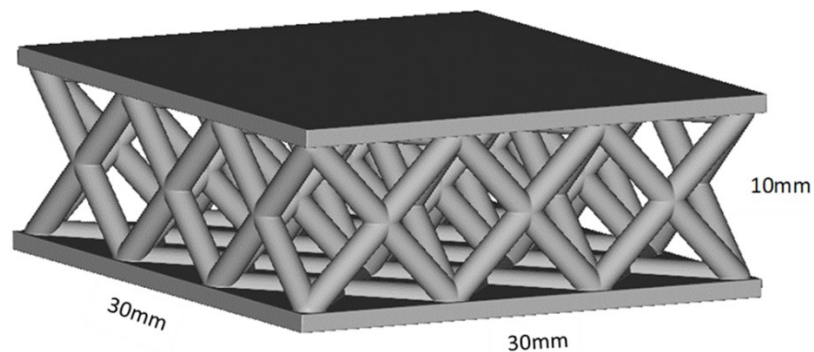


Figure 3.5: Example of a specimen build with the FCC unit cell.

Because the property of the lattice structure is different with varying topologies, the stiffness and the capability to reduce plantar pressure are also different in the specimens. The specimens are made with different cell sizes and strut diameters. Figure 3.6 show Diamond unit cell build with struts of 1mm. These parameters, considered together, constitute a fundamental element for the characterization of the specimens, once the capacities of the unit cells have been tested from a numerical point of view. The size of the cells and the diameter of the struts can define different density of the specimen, enable to create unit cells and so samples with different properties, such as stiffness, flexibility energy absorption.



Figure 3.6 Different views of the Diamond unit cell.

The dimensions of these parameters are chosen on the basis of the data considered by other works relating to footwear lattice structures and considering the guidelines of additive manufacturing. Even the constraints given by the printing process, in this case the SLS, have been taken into account (e.g., structures with thicknesses less than 1mm can be difficult to print). The study [44] used cell of 6mm and struct diameter of 0.6, 1, 1.4, 1.8 mm respectively for the creation of the insole. Another one [45] , presented conformal cell of variable sizes that adapted at the geometry of the shoe sole, and struct of variable diameter from 0.5 to 0.8. based on the type of the cells.

Based on these considerations, this study investigates samples with cells of different sizes: from 5 mm up to a maximum of 16 and 18 mm (depending on the topology that is used), to which we have assigned the following diameter of the struct: 1, 1.5 , 2 mm (Table 3.2).

Table 3.2 Samples realized for each unit cell topology.

UNIT CELL	CELL SIZE (mm)	STRUCT DIAMETER (mm)
BODY CENTERED CUBIC	5 - 6 - 7,5 - 8 - 9 - 10,5	1 - 1,5
SIMPLE CUBIC	5 - 6 - 7,5 - 8 - 9	1 - 1,5
DIAMOND	5 - 6 - 7,5 - 9 - 10,5 - 12	1 - 1,5 - 2
FACE CENTERD CUBIC	5 - 6 - 7,5 - 9 - 10,5 - 12 - 15 - 16	1 - 1,5 - 2
OCTET	6 - 7,5 - 10,5 - 12 - 15 - 16 - 18	1 - 1,5 - 2
FLUORITE	5 - 6 - 7,5 - 9 - 10,5 - 12 - 15 - 16	1 - 1,5 - 2

Specimens that have a relatively large cell size are also constructed and simulated, especially for those cell topologies that exhibited a more rigid behavior due to the greater density of the lattice structure, in order to observe their performance even at high degrees of porosity (Figure 3.7).

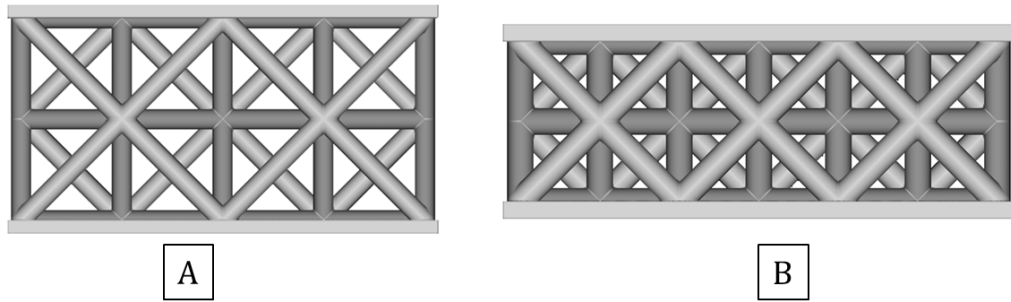


Figure 3.7: Samples characterized by Octet lattice topology with different sizes and same dimensions of struct diameter of 1,5mm. A) Cell size of 15 mm. B) Cell size of 9mm.

3.3 Material (TPU)

The material considered to manufacture the insole is the Thermoplastic polyurethane (TPU) given its good mechanical properties. This material has also been used by other studies that have modelled an insole with additive manufacturing with the aim of redistributing plantar pressure. The thermoplastic polyurethane is characterized by its high resistance to abrasion, wear, tear, oxygen, ozone and low temperatures. This combination of properties makes the thermoplastic polyurethane an engineering plastic. Used in the field of footwear is able to guarantee high performance and low weight shoe sole, which combines design, comfort and outstanding performance. This allows the product to reach excellent physical and mechanical properties while maintaining a light weight. In the same way, this product allows the development of any type of design, possessing high quality finishes. The TPU insole is introduced as a good alternative to the vulcanized rubber soles, since it has excellent qualities with a significant weight reduction (Figure 3.8).



Figure 3.8: Image of an insole manufactured with TPU material.

The advantages of the TPU include:

- Ultra-soft and flexible;
- Lightweight;

- Excellent physical and mechanical properties: good grip and excellent abrasion resistance;
- Shock Absorption;
- It allows working with inserts of welts, logos, and special pieces;

Consequently, also the specimens are manufactured in TPU, and its material properties (Table 3.3) are used in the modeling work. The SLS process is used for printing, which uses TPU powder particles to produce the desired object. Therefore, the properties of the TPU powders relating to the indicated printing technology have been considered, which differ from those of the TPU filament used in FDM printing techniques.

In particular, the young modulus of TPU powder is much higher (75MPa) than that of TPU filament (10/20 MPa) ; usually the TPU 95 A shore A is used for FDM printing, which tends to make the powder much more rigid than the filament thus producing more resistant and less elastic objects. The TPU powder offer a balanced property profile with good flexibility, shock absorption and the possibility to print very fine structures with a high level of detail.

Table 3.3 Material properties of the TPU powder for SLS printing

Density (g/mm ³)	Young's modulus (MPa)	Tensile stress Yield (MPa)	Hardness
0,00121	75	7	90 shore A

3.4 Boundary condition

The mechanical performances of the different samples are studied with numerical analyses, to evaluate the behavior of the different cells. Subsequently, the cells that exhibit the best behavior are selected and samples build with these printed. To simulate the contact mechanism existing between the foot and the insole, forces are made to act on the specimens, assuming that they are in a static condition and therefore neglecting the different walking activities, to which the insole would be subjected during the cycle of the gait .

To remake the foot-insole contact mechanism, the following forces are therefore considered for the simulation with the specimens:

- Vertical Downward Pressure (pressure exerted by the foot on the interface with the insole);
- Horizontal Pressure (shear force);
- Fixed Support by the lower plate.

The vertical pressure and the horizontal pressure are both applied on the upper surface of the superior plate (Figure 3.9). The horizontal pressure acts in the x direction.

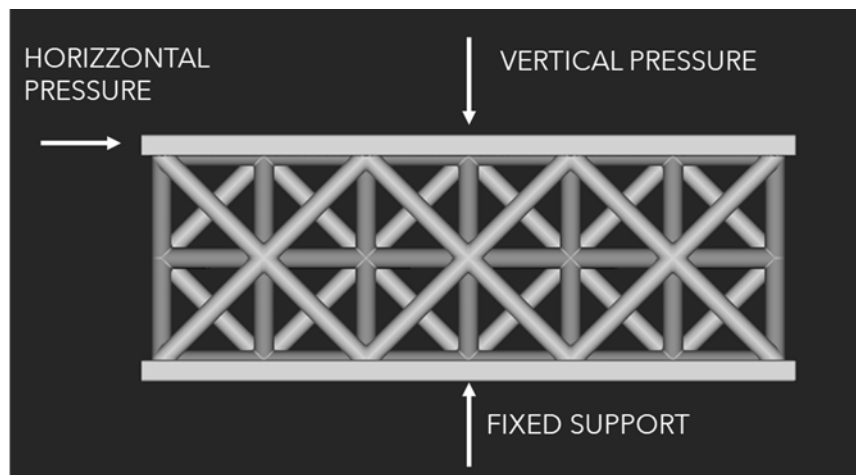


Figure 3.9 Boundary condition applied to the samples to perform the simulation.

Different intensities of loads has been simulated considering multiple levels to simplify the interpretation and to observe the behavior of the lattice, at multiple levels of stress (Table 3.4). It goes from a minimum value of 25 KPa for pressure and 10 KPa for shear to a maximum (peak) value of 6000 KPa for vertical pressure and 240 KPa for the shear.

Table 3.4: Different intensity of the loads simulated with the static analysis.

LOADS	1	2	3	4	5	6	7	8
Pressure (KPa)	25	50	100	150	225	300	450	600
Shear (KPa)	10	20	40	60	90	120	180	240

These stress values are selected from studies [47] that had investigated and experimentally measured the plantar pressure and shear in the different areas of the foot, with the various measurement methods, paying particular attention to the average and peak stress values and to the contact areas between foot and insole.

In the choice of loads , the dimensions of the specimens, on which these forces act, are taken into account, which are very small compared to the dimensions of a whole insole, thus, excessively high levels of load are not considered.

Once the numerical analysis with the specimens has been performed, from the comparison of the results, we can know which of the unit cells had a better and more suitable behavior to build the insole. Samples with best topologies, with cells of different sizes, are printed with SLS technology.

3.5 Insole

The last part of the study involves the creation of the insole with lattice material adopting the cell morphology selected by the analysis with the specimens.

The purpose is to create an insole with a non-homogeneous material, but modified internal lattice distribution, creating areas with different densities in order to alter the mechanical properties, to redistribute plantar stresses.

The study [45] proposed an iterative optimization method based on FE analysis-a new design method, for improving the stress distribution of the contact surfaces between the foot and the insole by applying functional gradient structural properties to the insole. The main idea of this method was to modify the material properties of various regions of the insole according to the FE predicted contact pressure value, so as to reduce peak pressure value and uniform the pressure distribution.

In a similar way this study tries to develop a method, to modify the material properties of various regions of the insole, as a function of contact pressure but also considering the plantar shear. For this purpose, it is necessary to have the distribution of pressure and shear in the foot given by the respective baropodometric maps (loading maps), to understand which areas of the foot are subjected to a greater load and therefore where it was necessary to lighten the insole to reduce stress.

The basic idea is to initially create the homogeneously distributed lattice structures inside the insole, using a certain unit cell topology. Then modify this distribution, decreasing the amount of lattice material in the areas subjected to greater pressure or shear load in order to make the structure lighter, and redistribute the material in the neighboring areas.

The CAD model of the insole must have a certain thickness, approximately 10 mm, so that it is possible to create a lattice structure inside it. To change the distribution of material inside it, it was superimposed on the stress maps, within the software used for modeling, in order to accurately visualize the different areas of the maps in the interior of the insole.

As we have already seen there are several CAD software that enable to model the insole with lattice structures. In this study the nTopology software is used.

4 Case study

4.1 Software: nTopology

nTopology is one of the most advanced engineering software for generative design and design tools for advanced manufacturing. Figure 4.1 represent the specific logo. With a diverse and unique toolset of generative design and automation capabilities, nTopology offers solutions to tackle the specific challenges of any industry, from automotive, medical until aerospace. Generative design is a broad and holistic design methodology. It includes all goal-driven and computational approaches to engineering that use software to generate geometry based on a set of logical operations and user-defined rules. In other words, generative design is a set of digital tools that augment your capabilities as an engineer and designer. These tools address the main engineering need for exploring efficiently and effectively the entire available design space. This enables to converge quickly to the best possible solution that meets all design requirements – both technical and non-technical.



Figure 4.1: nTopology logo.

The main functionalities and capabilities of the software are the Topology Optimization, the Simulation process, and the creation of advanced lattices in a short time, to minimize weight and material usage, improve energy absorption and the heat exchange.

The multiple tools offered by the software (platform) can be grouped into some main submenus:

- Create and Modeling: tools intended for the realization of solids and their modeling (orientation on the construction plane, Boolean operations, translations, mass calculation etc.);
- Lattices & lightening: useful tools for the realization of lattice structures and operations with these structures with the aim of significantly reducing the weight of the component under examination;
- Simulation: tools that allow you to establish the boundary conditions of the component (constraints, applied forces and moments, thermal loads, etc.) and to carry out various types of analysis (analysis static, thermal, modal etc.);
- Design Analysis: this menu offers the possibility to choose a specific material within a large database and there are also numerous tools dedicated to the creation of meshes and their modeling (Remesh Surface, Refine Mesh etc.);
- Topology Optimization: tools dedicated to optimization; give the possibility to choose the goal of topological optimization, for example the reduction of deformations caused by the applied loads, but also to impose constraints on the optimization process (Volume Fraction Constraint, PassiveRegion Constraint, Planar Symmetry Constraint, Extrusion Constraint etc.).

With nTop Platform's Field-Driven Design, you can use biometric measurements or other experimental data captured in the lab to directly drive and control advanced geometry. For example, the pressure map of a foot can directly controls the density of the lattice density of a midsole. This enables the design of products with superior performance and unlocks mass design customization using nTop Platform's reusable workflows.

This special application is used in the following study to model the insole and to modify the distribution of the lattice structures.

In particular, the nTop platform is used first to characterize the various unit cells with the use of specimens subjected to certain stress conditions, and then to design the insole with lattice structures.

4.2 Cells characterization

The first part of the study is dedicated to the study of unit cells. To do this, the specimens are created with lattice structures of the selected topologies and analyzed with the FEA, within the nTop platform.

4.2.1 Creation of Lattice Body

The first step inside the platform is the creation of the solid to be filled with the lattice, and two other solids corresponding to the two plates that delimited the design space. This is done using the command 'Box' inside the tools 'Create' and entering the dimensions and the positions for the solids. The dimensions of the plates and of the central box are made considering the sizes of the cells of the lattice structure.

Figure 4.2 show the procedure to build the rectangular box with the relative plates (Figure 4.3).

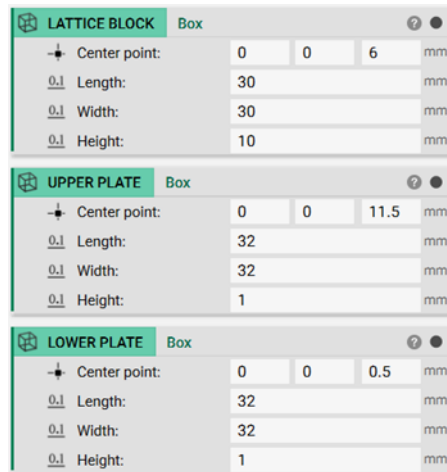


Figure 4.2: Creation of rectangular box that delimit the design space.

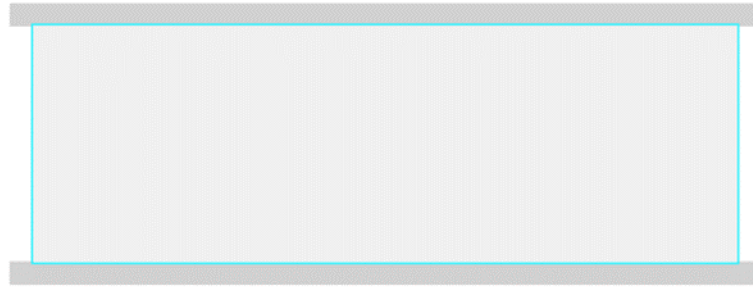


Figure 4.3: Box that define the specimen dimension.

The next step consists in building a map of rectangular cells in the space provided for the lattice, using the command 'Rectangular Cell Map'(Figure 4.4). This tool allows to define the dimensions of the cells, which in our case are homogeneous in all directions, and the unit cell with which fill the lattice and that will be repeated within the structure. In Figure 4.5 a cell map with cell of 10mm has been designed in the design space.

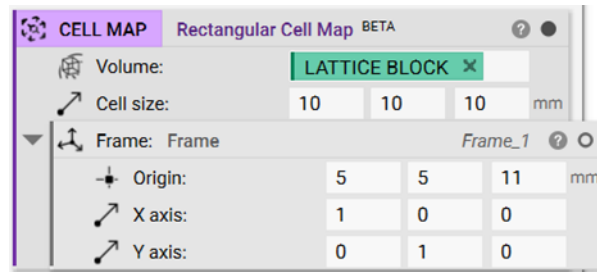


Figure 4.4: Creation of rectangular cell map.

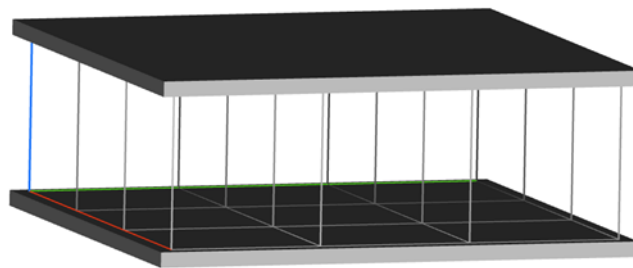


Figure 4.5: Cell map realized with cell dimension of 10mm.

At this point the lattice body is generated with the function 'Periodic lattice body' which tessellates the unit cell selected through the periodic map and enable to define the diameter of the structs for the lattice material. In the following example the face Center Cubic unit cell is adopted with 1mm diameter of the struct (Figure 4.6).

Then the 'Boolean union' is performed to join the lattice structure with the upper and lower plates and obtain a unique body (Figure 4.7).

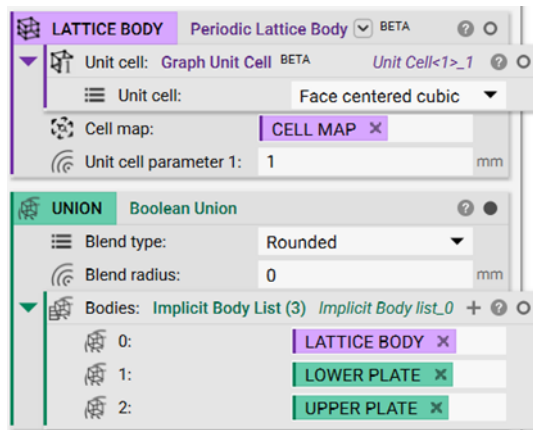


Figure 4.6: Lattice body creation inside the cell map, specifying the lattice topology.

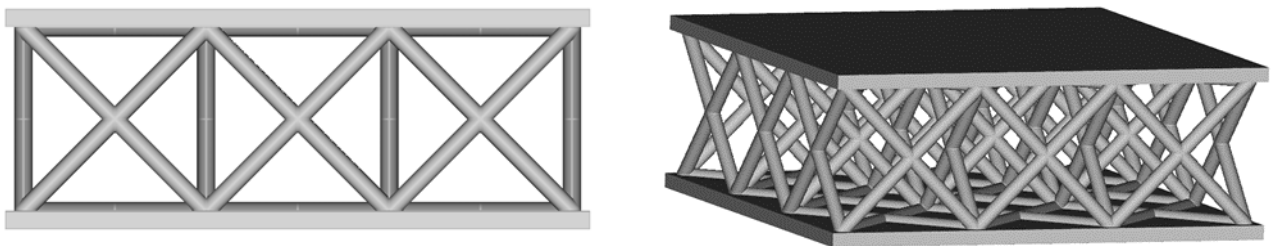


Figure 4.7: Sample with FCC unit cell and struct diameter of 1mm.

4.2.2 Finite element model generation

The second step is to convert the implicit body of the specimen into the finite element model by generating the mesh for carry out the static analysis. The component surfaces are discretized by creating a mesh.

Thanks to the tools ' Mesh from implicit body' the surface mesh is realized; the tools 'Refine Mesh' is used to maximize the precision of the created grid. In this phase it is important to make attention to the size of the mesh, as the denser the network of triangles that discretizes the surfaces of the component, greater will be the degree of precision. Then, using the 'FE Volume Mesh' tool, the volume mesh is created. In this study we set the mesh size to 0.5mm. (Figure 4.8-Figure 4.9)

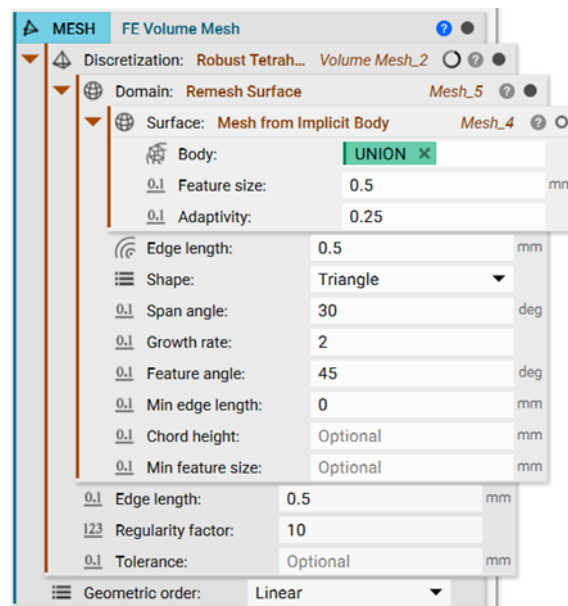


Figure 4.8 Creation of the Mesh to define the finite element model for the simulation.

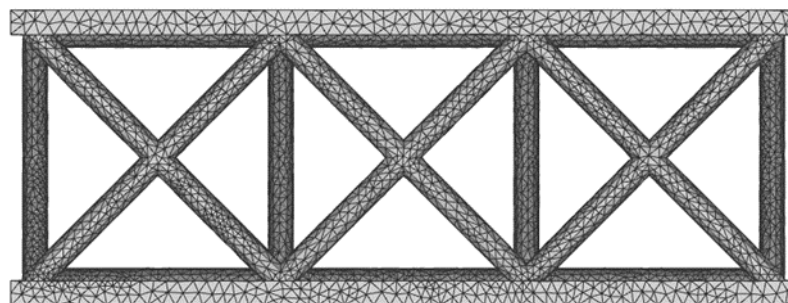


Figure 4.9: Mesh of the specimen.

At this time the material properties of the body are defined. NTopology has a large database of materials to draw from, but if the material to be used is not present in the list, the 'Isotropic Material' block can be used, inside which the properties of the material must be manually specified: modulus of elasticity (modulus Young's), transverse contraction coefficient (Poisson's ratio), density, etc. In this study the material used is TPU powder considered for SLS 3D printing , therefore the properties entered are: Young's Modulus of 75MPa and a Poisson's ratio of 0,4 (Figure 4.10).

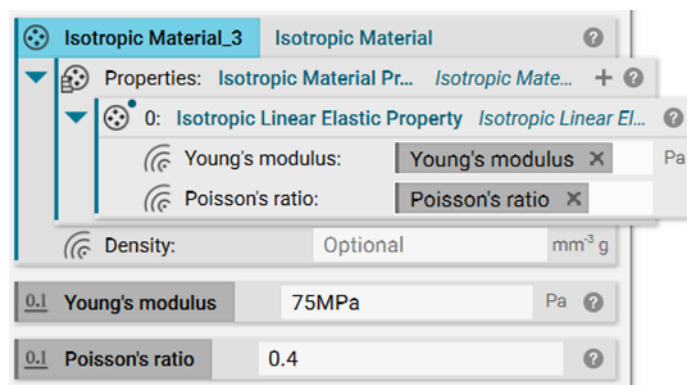


Figure 4.10: Set the Material Properties for the specimen.

4.2.3 Static analysis

The third step is that of static analysis. Calculate displacements, strains, stresses, and reaction forces of an FE Model under the effect of applied boundary conditions. Boundary conditions of the component under examination are defined. More precisely, the values of the external loads are defined (force, pressure, applied moment etc.) and the element of the component on which these acts. In a similar way, the constraint conditions are also established through the 'Displacement restraint' command, for those surfaces that must not undergo displacements and variations in geometry following the application of external loads.

From the static analysis it is possible to extract the displacement and stress values which will be used for the evaluation of the cells. In this case (Figure 4.12) the maximum load condition considered by the study is simulated. A vertical pressure of 150 KPa and a shear force of 61N (calculated on the surface area of the plate) act on the superior plate (Figure 4.11). The software does not allow to generate horizontal pressures; with the 'Pressure' command only vertical stresses can be generated. Therefore for the simulation of the shear stress an horizontal force is generated calculated for the area of the plate where act. With the 'displacement constraint' command and selecting the bottom plate, the lower plate is constrained.

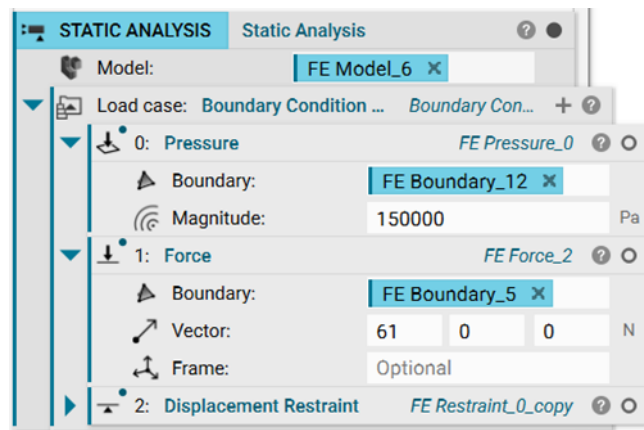


Figure 4.11: Define Boundary condition to perform the static analysis.

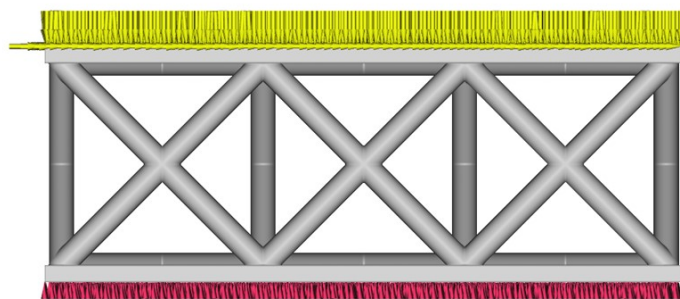


Figure 4.12: Application of Boundary conditions.

4.3 Insole modelling

The second part of the study is aimed to creating the internal lattice of the insole using the unit cells selected from the analysis with the specimens and modifying the distribution of the material to reduce internal stresses.

4.3.1 Cad model

The first step consists in importing the CAD file of the insoles into nTop platform using the "Import Part" tool. The 3D model of the insole (Figure 4.13) is selected from a previous study within the university.

Since the original imported model was extremely thin (about 3 mm), in order to generate an orthopedic insole with internal lattice it is necessary to have a thicker insole. Therefore, by using the Rhinoceros6.0 software, the thickness of the insole has been increased, reaching 10mm in the forefoot area until to 18mm in the lateral parts of the heel.

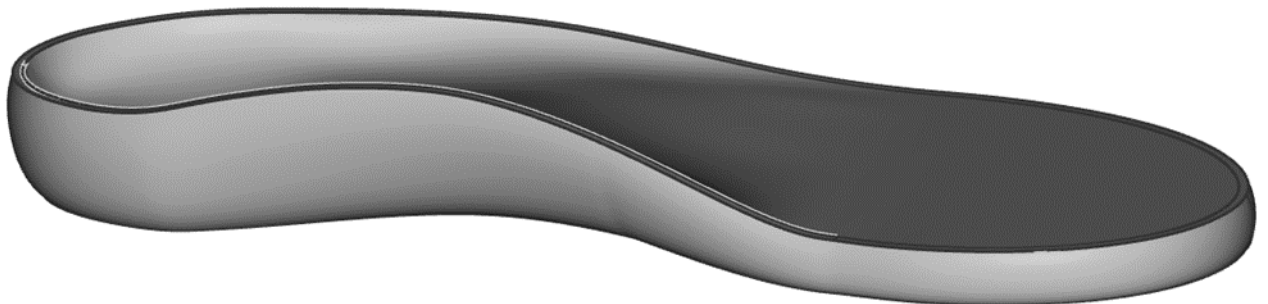


Figure 4.13: Cad model of the insole.

Once the model has been imported, it is converted into an implicit body through the 'Implicit Body from Cad body' command to allow modeling. Then the definition of the surfaces is performed; in particular, the upper surface and lower surface of the insole are defined, which delimit the space where the lattice will be created, and a thickness is assigned to them (in this case of 1 mm) to transform them in solid bodies (Figure 4.14).



Figure 4.14 : Upper and lower layer of the insole.

4.3.2 Baropodometric maps

The second step refers to the load maps to be used to create the lattice structures. These should be measured in a laboratory with the appropriate instruments (platform or wearable sensor), but due to the impossibility of making such measurements, they were taken from other sources. The pressure map is selected, as for the insole, from a previous study at the university (Figure 4.15). The plantar shear map (Figure 4.16) was taken from a study available in Pubmed, which investigating plantar stresses[46].

These are imported into nTop platform using the 'Import scalar point map' command, which imports the scalar point map from a CSV file, where the different points are specified by the x, y, z coordinates (that indicate the spatial position within the map) and a value 's' relative to the value of the pressure or shear. Since that originally the maps are image files, to carry out this conversion the Rhino software is used, which, thanks to the 'Heightfield' command, allow to map the points, creating NURBS surfaces from grayscale values of the colors image file. Then by extracting the points of the map and assigning them values in relation to the considered pressure range (0-150KPa for the Pressure, and 0-60Kpa for the shear), it is possible to obtain the map in the desired format. Always inside Rhino, the maps have been translated and scaled according to the insole, in order to match the points of the map with specific areas of the insole, since the source of the files are different.

Then using the 'Field from point map' tools in nTopology, a scalar field is created from the pressure point map which will be used in the final phase of the study.

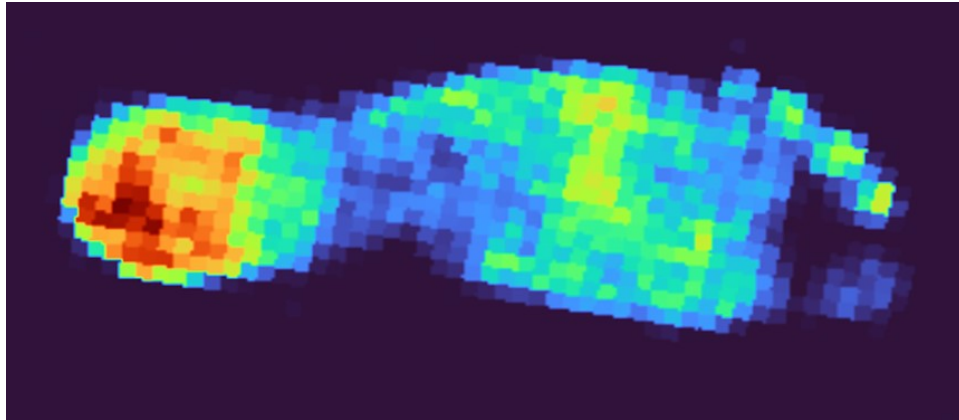


Figure 4.15: Pressure Map.

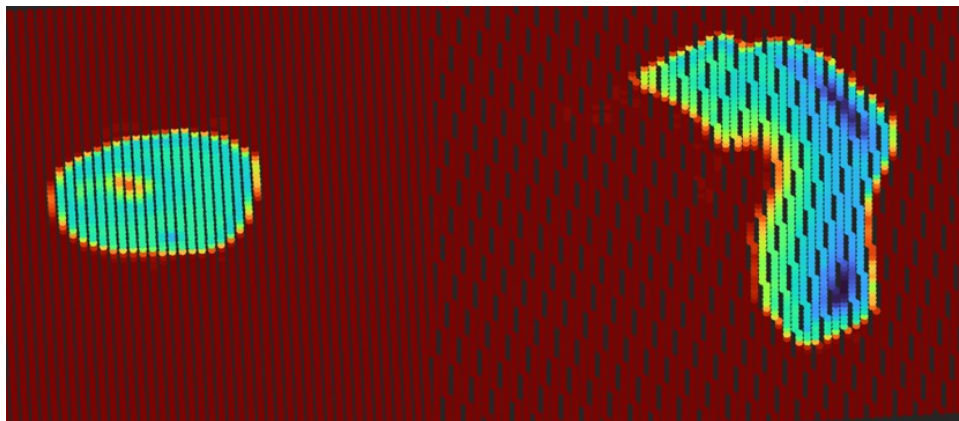


Figure 4.16: Shear Map.

4.3.3 Insole filling with lattice

The last step is the creation of the lattice structure inside the insole and the changing of the material properties according to the distribution of plantar stresses. There are two different ways with the software used, through which it is possible to modify the density of the lattice based on the regions of the map where there is a different intensity of load. In the first method the sizes of the single cells that make up the lattice are modified, leaving the diameter of the struts unchanged. Instead in the second method, the dimensions of the cells remain unchanged but the diameter of the struts is altered to create a lattice with variable density.

In both cases we start by creating a rectangular cell map, as we did for the specimens, using the 'Rectangular Cell Map' block, indicating the insole as the body where to create this map, and specifying the size of the cells that compose it. In this case the cells are 13 mm (Figure 4.17).

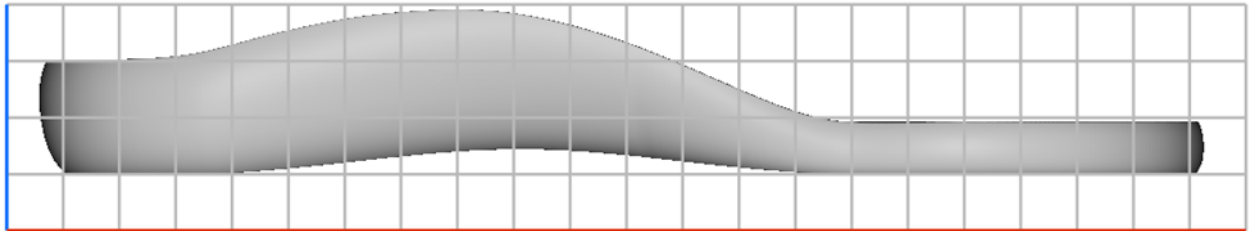


Figure 4.17: Cell Map for the insole model.

Both methods use the 'Ramp' block to change the density and distribution of material, but in different way. Unfortunately, the software doesn't allow to vary the distribution of material according to both loads (pressure and shear), ie it does not allow the use of both maps at the same time but only one can be considered to vary the lattice structure. The Ramp block allows to scale values from one range, within the input min and max, to its relative value within an output range. The ramp process can be performed on singular scalar values, or entire scalar fields. When ramping with scalar fields, we're able to take the qualitative shape of an input field and give it new quantitative values. Ramping can be used in conjunction with any block that accepts a scalar field input in order to make the effect of that block spatially varying.

In the first case the 'Ramp' tool is used to change the size of the cells. In this case the scalar field of the pressure map is entered as input with the relative min and max values (which delimit the range of the pressure variations) and as output a scale factor (dimensionless) which represents the output variation and in this case the cells size variation.

Therefore in 'Out min' which represents the output value where there is a lower pressure value, 1 is entered, because the size of the cells must not change (you can also enter a negative value, such as -1, in this case we will have a narrowing of the cells), while in out max which represents the points where the pressure is greater, enter 2 (in this way an enlargement of the cell in these points is obtained). Therefore, with these values, a cell of double size at the peak points will be obtained, which gradually decreases as it moves towards the points of lower pressure. The greater the difference between the values of out min and out max, the greater the deformation of the cells (Figure 4.18).

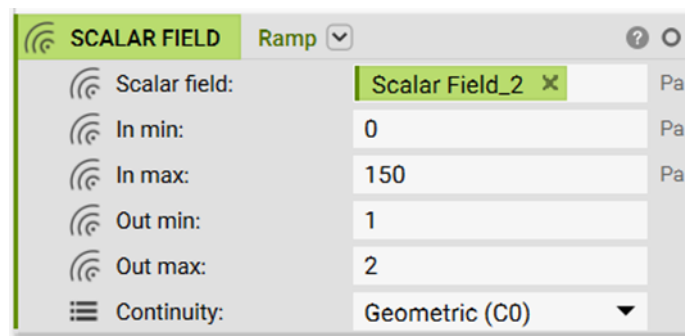


Figure 4.18 Ramp block for modify cells size.

Then using the 'Warp cell Map' block (Figure 4.19) is possible to deform the cell map. In input, the original cell map, is entered and even a discretization factor that serves to determine the number of points of the grid of the cells on which the transfer function will be calculated; the higher it is, the more detailed will be the modified map. The warp block is composed by three scale factors corresponding to the three directions. Here the ramp block is inserted on all fields, until the map deforms according to the created ramp, in all directions (Figure 4.20).

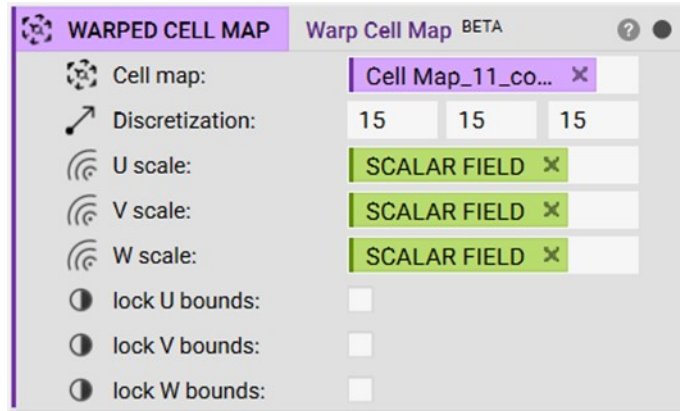


Figure 4.19 Map deformation based on the pressure level

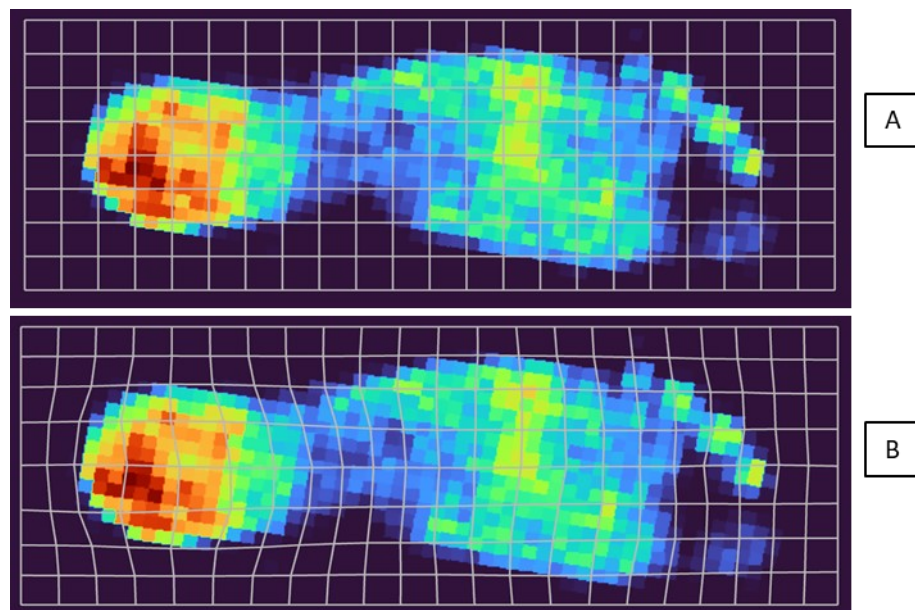


Figure 4.20 A) Original cell map. B) Warped cell map.

Once the cell map has been modified, using the 'Periodic Lattice Body' block, the lattice structure is generated inside the map, specifying the unit cell topology with which fill the map and the size (diameter) of the struct, that in this case will be constant.

Finally, using the tool 'Boolean Intersect' (create an implicit body where the input bodies spatially overlap) between the created lattice structure and the implicit body of the insole, an insole is created containing only lattice structures. In Figure 4.21 the Octet unit cell has been used to realize the insole with the diameter of the struct of 1,5mm.

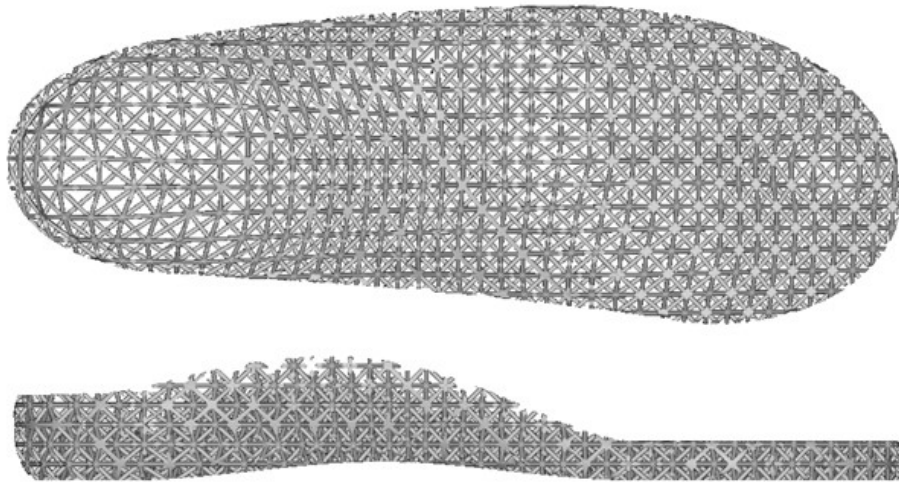


Figure 4.21 : Insole lattice realized with variable cells size.

In the second case, instead, the Ramp command is used to vary the size of the struct of the lattice. Therefore, as output values (out min and out max) we must enter the minimum and maximum size of the desired struct. In this way, where there will be a higher pressure, the structures will have a smaller diameter creating more porous cells, to relief plantar stress. Where the pressure will be lower the cells will be denser due to a larger diameter of the struct. In figure the diameter of the structs varies from 1mm where the pressure was greater, creating a lighter structure, up to 2mm, in the areas subjected to less pressure that did not require lightening (Figure 4.22).

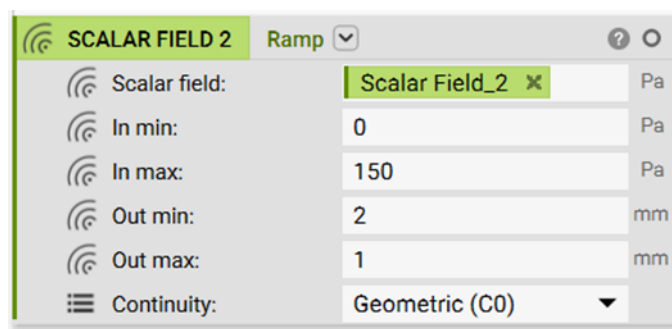


Figure 4.22: Procedure to modify the struct diameter.

Even in this case, the lattice structure is created using the 'Periodic Lattice Body' block and specifying the topology of the cell. But this time the diameter of the structs will not be fixed but vary according to the pressure map, thus according to the ramp created (Figure 4.23).

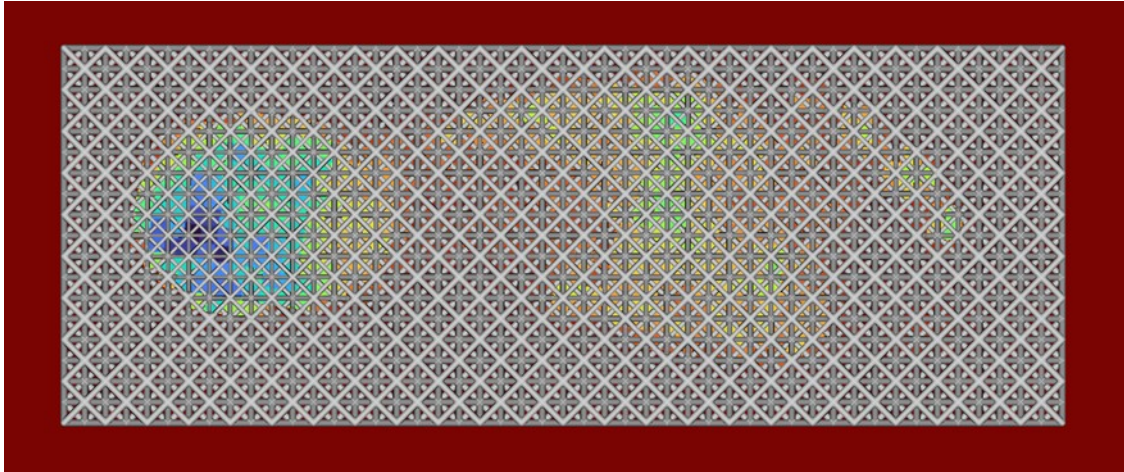


Figure 4.23: Lattice map with variable struct diameter in function of the pressure map.

Therefore, the ramp block is entered as a variable to determine the diameter of the structs. Then using the 'Boolean intersect' the insole lattice is generated.

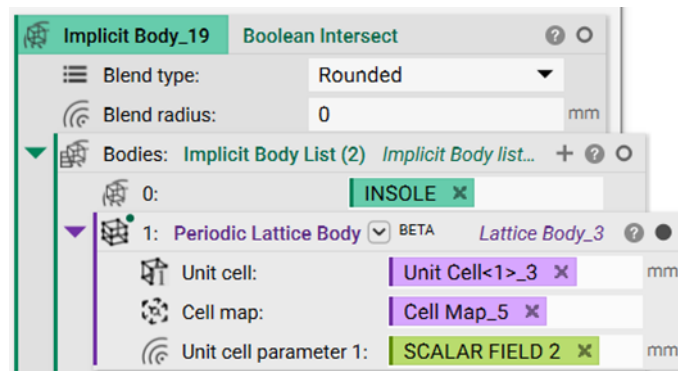


Figure 4.24 : Command to create lattice body inside the insole.

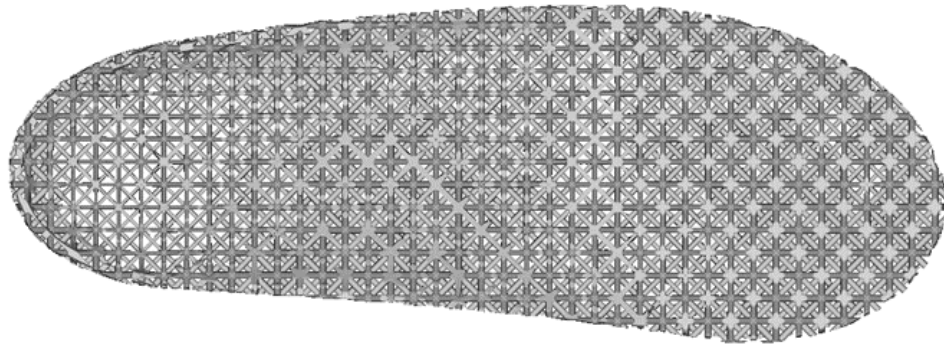


Figure 4.25: Lattice insole with variable structs dimension.

The last step, the same for the two types of insoles made, is the 'Boolean Union' between the lattice body and the two layers of 1mm thickness, defined in the initial part of the insole modeling. These are added on the upper and lower surface of the insole and represent the surfaces in contact with the foot on one side and with the shoe sole on the other, to prevent stress concentration and improve the quality of the surface (Figure 4.26).

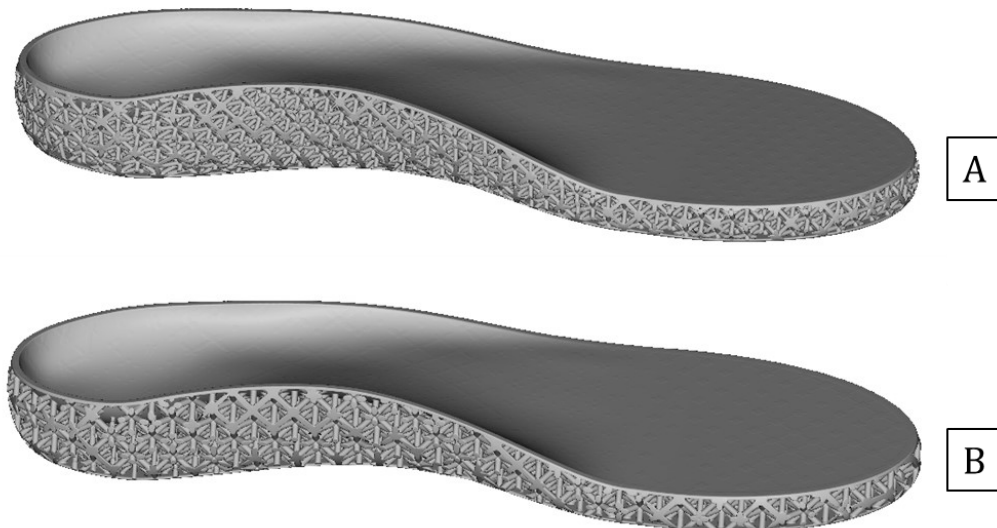


Figure 4.26: Final insole models created with the two ways. A) Insole built by using the octet topology, deforming the cells from 9 to 18 mm and keeping the diameter of the struct constant to 1,5 mm. B) Insole constructed using octet topology, cell size fixed at 12 mm and struct diameter ranging from 1 to 2 mm.

5 Result & Discussion

The static analysis with the specimens, enable to characterize the unit cells. The static analysis calculates the displacements, stresses, strains, and reaction forces of an FE Model under the effect of applied boundary conditions.

In this study, the output parameters used to evaluate and compare the various cell topologies are the horizontal and vertical displacement (evaluated on the middle of the top surface), and the Von Mises Stress (the maximum value). These results are evaluated taking into account the density of the structures to understand which of them best reassigned the efforts within the sample. The stiffness has also been calculated, both for the tangential and for the vertical forces, determined by the ratio between intensity of the load applied for the vertical or horizontal deformation depending on the type of stress considered. As expected, as density increased, the stiffness of the sample increased.

Figure 5.1 show the static analysis of a specimen build with the octet unit cell, with 12 mm cells and 1.5 mm struts diameters when the maximum load intensity is applied.

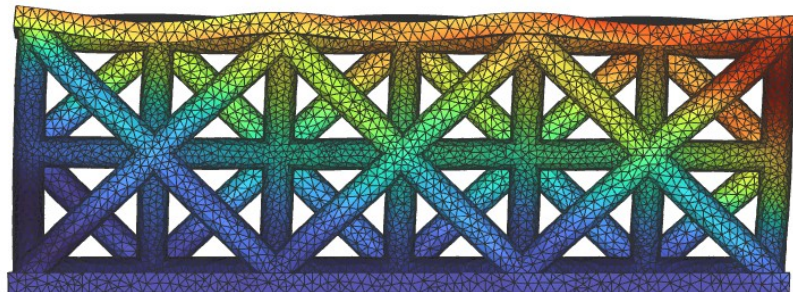


Figure 5.1 Static analysis of a sample build with FCC unit cell, subjected to the maximum intensity of loading. Deformation of the specimen is displayed.

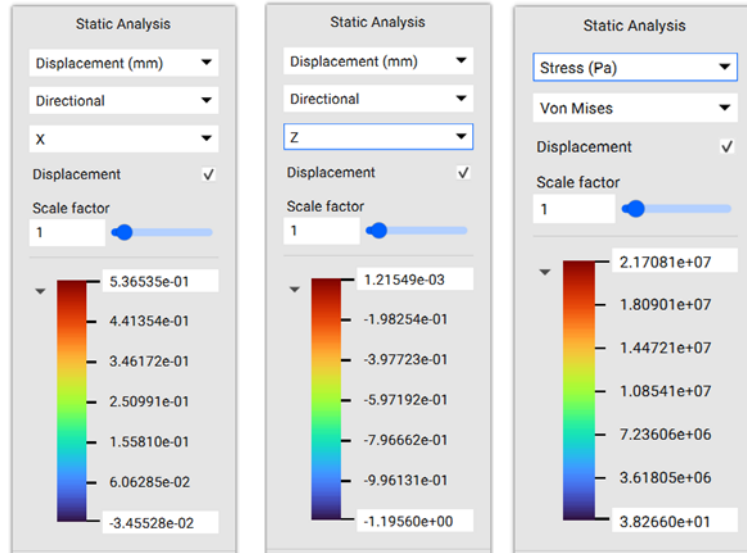


Figure 5.2: Results of the analysis. A) Horizontal displacement. B) Vertical displacement. C) Von mises stress.

Table 5.1 shows the results of the simulation, for the different unit cells topologies, obtained by applying the maximum intensity of pressure and shear to a sample with 6 mm cells and a strut diameter of 1.5 mm. The output parameters considered to compare the unit cells with each other are also calculated as a function of the lattice density, for the corresponding cell, to evaluate how this measurement influenced the behavior of the cells. The following lattice topologies are also compared using the other dimensions of the specimens, yielding the same results in terms of comparison between the single unit cells.

Table 5.1: Static analysis results for cell topology at 6mm cell size and 1,5 struct diameter.

UNIT CELL TYPE	CELL DIMENSION (mm)	STRUCT SIZE (mm)	HORIZONTAL DISPLACEMENT (mm)	VERTICAL DISPLACEMENT (mm)	RELATIVE DISPLACEMENT (X/Z)	VON MISES STRESS (Pa)	DENSITY	DISPLACEMENT X * DENSITY	DISPLACEMENT Z * DENSITY	VON MISES STRESS * DENSITY
BODY CENTER CUBIC	6	1,5	1,81	1,88	0,96	1,69E+07	42%	0,75	0,78	7,05E+06
FACE CENTER CUBIC	6	1,5	1,18	0,91	1,30	9,64E+06	48%	0,57	0,44	4,66E+06
SIMPLE CUBIC	6	1,5	11,98	1,91	6,27	3,15E+07	34%	4,03	0,64	1,06E+07
DIAMOND	6	1,5	1,72	1,28	1,34	1,29E+07	42%	0,72	0,53	5,36E+06

OCTET	6	1,5	0,50	0,35	1,43	4,61E+06	65%	0,33	0,23	3,00E+06
FLUORITE	6	1,5	0,70	0,46	1,52	9,68E+06	56%	0,39	0,26	5,43E+06

This table shows the results of the static analysis of the various unit cells relating to a certain size of the cell (6mm) and a certain diameter of the structs (1,5mm). The complete table containing the results for all tested specimens is in the Appendix section at the end of the study (Table 8.1). In particular, the analysis highlighted the following properties for the different unit cells.

The Body Centered Cubic unit cell has the highest level of vertical displacement, which makes it the best topology for releasing vertical pressure and ensuring good energy absorption. However, it generates a high level of internal stress, producing bad results in term of tension distribution. The Simple Cubic topology shown the largest horizontal displacement caused by the application of the horizontal component of the pressure. For this reason, it is particularly suitable for reducing the plantar shear ensuring good lateral cushioning, even if the lateral deformation, when the maximum load is applied, turns out to be excessive, almost unreal, as can be seen from the simulation results. In contrast, this topology presents an extremely high value of internal stress related to the density. These results suggest, not considering this topology as specifically proper for filling the insole to allow redistribution and offloading of tension.

The Octet has the minimum displacement, when it is subjected to an external load, therefore it is the most rigid structure to tangential and vertical loads among all those considered. However, it also presents the lowest level and more uniform distribution of stress, relating to the density, producing the best distribution of the material and maximizing the ratio between stiffness and density. This guarantees a better fatigue behavior and improved stiffness.

The Diamond unit cell presents an intermediate behavior between that of the other structures generated, without highlighting any particular properties in comparison with the other unit cells. To conclude the Face Centered Cubic and Fluorite topologies have a low level of stress, and good results with behavior similar to that of the Octet topology.

From these results it can be deduced that that the Octet topology has the best behavior, since it minimizes the level of internal stress in the peak area, redistributing it in the adjacent regions, followed by the Fluorite and Face Centered Cubic topologies. Octet has the highest degree of stiffness followed by Fluorite and FCC. Therefore, for experimental evaluation and 3D printing of the specimens these three unit cells, are considered.

Taking the table of results (Table 5.1), it is possible to observe that these cell topologies presented a high level of density which make them more rigid to tangential and vertical displacements, as well as having a good distribution of stresses. However, due to their high rigidity, these structures are not particularly characterized with good energy absorption capacity.

For this reason, to select the size of the samples to be printed, those with a lower material density are chosen in order to reduce stiffness and increase energy absorption. In fact, as it is possible to observe by comparing different dimensions and therefore density of the same unit cell, Table 5.2, reducing the amount of material inside the structure, increased the deformation of the lattice (greater damping effect).

Table 5.2 : Comparison static analysis results for cell at different density. Unit cell of 5mm with struct size of 1 and 1,5mm.

UNIT CELL TYPE	CELL DIMENSION (mm)	STRUCT SIZE (mm)	DENSITY	HORIZONTAL DISPLACEMENT (mm)	VERTICAL DISPLACEMENT (mm)	RELATIVE DISPLACEMENT	VON MISES STRESS (Pa)
BODY CENTER CUBIC	5	1	32%	2,03	2,16	0,94	2,64E+07
FACE CENTERED CUBIC	5	1	36%	1,47	1,15	1,28	1,54E+07
SIMPLE CUBIC	5	1	26%	21,15	2,21	9,57	8,09E+07
DIAMOND	5	1	32%	2,22	1,69	1,31	3,06E+07
OCTET	5	1	49%	0,62	0,49	1,27	7,90E+06

FLUORITE	5	1	42%	0,90	0,66	1,36	1,54E+07
BODY CENTER CUBIC	5	1,5	45%	0,77	0,68	1,13	1,63E+07
FACE CENTERED CUBIC	5	1,5	53%	0,58	0,38	1,53	5,57E+06
SIMPLE CUBIC	5	1,5	33%	4,89	0,97	5,04	2,16E+07
DIAMOND	5	1,5	45%	0,70	0,52	1,35	7,74E+06
OCTET	5	1,5	72%	0,23	0,15	1,53	3,03E+06
FLUORITE	5	1,5	62%	0,30	0,19	1,58	3,83E+06

Therefore, samples characterized by a greater porosity of the lattice are selected, i.e., which presented cells with a high ratio between cell size and diameter of the struts. As a consequence, samples with a denser lattice are discarded, such as where the ratio of cell size to structure diameter was less than or equal to 5.

The samples classified according to the type of unit cell are ordered for simplification, according to the diameter of the struts and for each of these different cell sizes were identified. For a certain lattice topology and a certain thickness of the struts, only the samples with the minimum and maximum cell size and for some, also an intermediate cell sizes are selected for printing, for a total of 19 samples (Table 5.3).

Table 5.3: Printed specimens.

STRUCT DIAMETER (mm)	1,5				1			2		
	7,5	9	15	18	7	8	10	12	16	18
CELL SIZE (mm)	7,5	9	15	18	7	8	10	12	16	18
OCTET		✓	✓	✓	✓		✓	✓		✓
FLUORITE	✓		✓		✓	✓		✓	✓	
FCC	✓		✓		✓	✓		✓	✓	

The results of the static analysis for the printed specimen are reported in Table 5.4. The complete table containing the results for all test specimens is in the Appendix section at the end of the study.

Table 5.4: Static analysis results of the printed samples.

UNIT CELL TYPE	STRUCT SIZE (mm)	CELL DIMENSION (mm)	DENSITY (%)	NORMAL PRESSURE (KPa)	SHEAR FORCE (N)	HORIZONTAL DISPLACEMENT (mm)	VERTICAL DISPLACEMENT (mm)	RELATIVE DISPLACEMENT (X/Z)	VERTICAL STIFFNESS (MPa)	HORIZONTAL STIFFNESS (MPa)	VON MISES STRESS (Pa)
OCTET	1	7	41	150	61	0,26	0,20	1,30	6,75	8,09	1,40E+07
OCTET	1	10	28	150	61	0,83	0,79	1,05	2,28	2,37	2,98E+07
OCTET	1,5	9	44	150	61	0,28	0,20	1,40	8,25	7,78	8,74E+06
OCTET	1,5	15	24	150	61	1,39	1,31	1,06	1,91	1,41	2,19E+07
OCTET	1,5	18	19	150	61	1,71	2,37	0,72	1,27	0,96	4,95E+07
OCTET	2	12	39	150	61	0,22	0,27	0,81	7,78	7,30	9,49E+06
OCTET	2	18	23	150	61	0,93	1,24	0,75	2,42	1,73	2,47E+07
FLUORITE	1	7	37	150	61	0,51	0,29	1,76	4,66	4,12	4,15E+07
FLUORITE	1	8	31	150	61	0,77	0,53	1,45	2,83	2,40	4,92E+07
FLUORITE	1,5	7,5	46	150	61	0,18	0,13	1,38	10,96	10,93	1,93E+07
FLUORITE	1,5	15	20	150	61	5,56	3,40	1,64	0,75	0,35	2,09E+08
FLUORITE	2	12	33	150	61	0,44	0,41	1,07	5,12	3,65	3,10E+07
FLUORITE	2	16	23	150	61	2,70	1,96	1,38	1,38	0,66	6,94E+07
FCC	1	7	34	150	61	0,55	0,45	1,22	3,00	3,82	2,94E+07
FCC	1	8	28	150	61	0,68	0,75	0,91	2,00	2,72	3,61E+07
FCC	1,5	7,5	41	150	61	0,27	0,22	1,23	6,48	7,29	1,30E+07
FCC	1,5	15	19	150	61	2,37	3,27	0,72	0,78	0,83	7,03E+07
FCC	2	12	29	150	61	0,47	1,10	0,43	1,91	3,42	4,44E+07
FCC	2	16	21	150	61	1,43	2,05	0,70	1,31	1,22	4,53E+07

For some of the selected specimens the behavior is studied considering different and even very high loads to observe how these behaved from the point of view of deformation and internal tension when the pressure change, until to hypothesize a high value of 600 KPa (Table 5.5). An important aspect is to see if the specimen collapses at a certain level of pressure or continues to deform gradually.

Table 5.5: Results of the analysis at different intensity of loads.

UNIT CELL TYPE	STRUCT SIZE (mm)	CELL DIMENSION (mm)	NORMAL PRESSURE (KPa)	SHEAR FORCE (N)	HORIZONTAL DISPLACEMENT (mm)	VERTICAL DISPLACEMENT (mm)	RELATIVE DISPLACEMENT	HORIZONTAL DEFORMATION	VERTICAL DEFORMATION	VON MISES STRESS (Pa)
OCTET	1,5	15	150	61	1,39	1,31	1,06	8%	4%	2,19E+07
OCTET	1,5	15	225	90	2,11	1,97	1,07	12%	7%	3,22E+07
OCTET	1,5	15	300	120	2,74	2,67	1,03	16%	9%	4,36E+07
OCTET	1,5	15	450	180	4,11	3,95	1,04	23%	13%	6,56E+07
OCTET	1,5	15	600	240	5,48	5,26	1,04	31%	18%	8,75E+07
FLUORITE	2	16	150	61	2,70	1,96	1,38	11%	8%	6,94E+07
FLUORITE	2	16	225	90	3,98	2,90	1,37	16%	12%	1,04E+08
FLUORITE	2	16	300	120	5,32	3,90	1,36	22%	16%	1,38E+08
FLUORITE	2	16	450	180	7,98	5,92	1,35	33%	23%	2,07E+08
FLUORITE	2	16	600	240	10,60	7,86	1,35	44%	31%	2,76E+08
FCC	2	16	150	61	1,43	2,05	0,70	11%	4%	4,53E+07
FCC	2	16	225	90	2,17	3,10	0,70	17%	6%	6,77E+07
FCC	2	16	300	120	2,90	4,13	0,70	23%	9%	9,03E+07
FCC	2	16	450	180	4,23	6,26	0,68	35%	12%	1,35E+08
FCC	2	16	600	240	5,60	8,10	0,69	45%	16%	1,81E+08

The results demonstrate that even at elevated loads the specimens always exhibit linear behavior in terms of displacement but also of internal stress. As can be seen from the strain-stress graph for perpendicular deformation, as the normal pressure increases, the vertical deformation grows steadily (Figure 5.3).

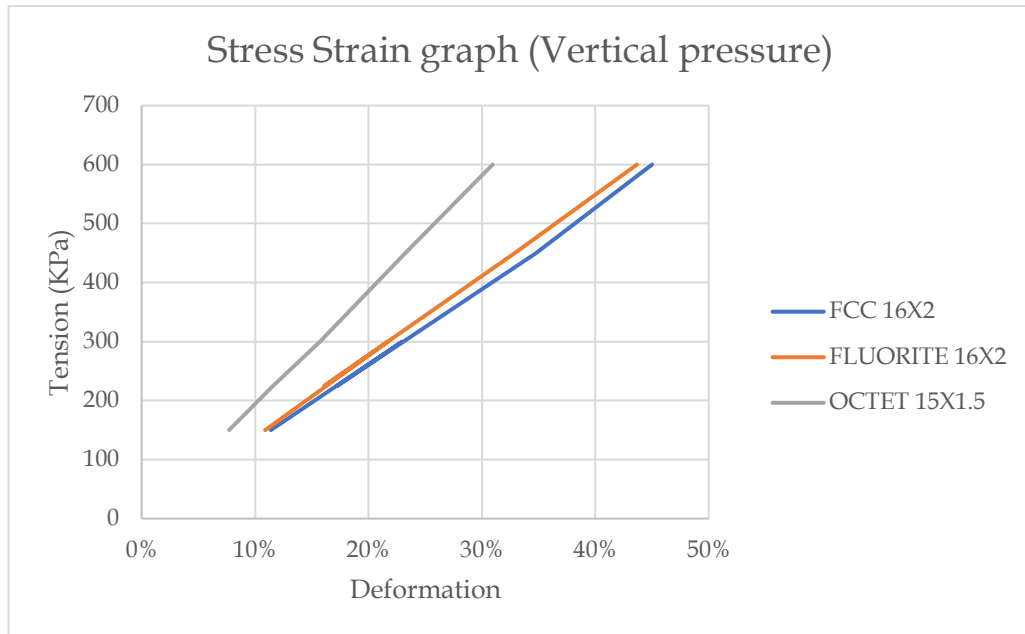


Figure 5.3: Stress strain curve for three different specimens.

The printed specimens (Figure 5.5, Figure 5.6, Figure 5.6) confirmed the results of the numerical analysis; the reticular topology of the Octet is more rigid and resistant, while the others are a little less. Similarly, specimens with cells of smaller dimensions are much harder and resistant to deformation while those larger ones such as 15/18 mm, bend easily.

Even the insole created by varying the lattice structure and cutting the cells has given good results even if the slicing of the cells in different points makes it lose the property that characterizes it. Printed specimens with the SLS process, have good component qualities and high detail accuracy.

Therefore, even for the possible processing of the insole, the SLS can be considered, and a high precision object is expected. This technique has proved to be a good low-cost printing process (among the cheapest), for objects of high quality,

NTopology has demonstrated good creation and processing skills with lattice structures and an interesting method to control advanced geometry using biometric measurements.

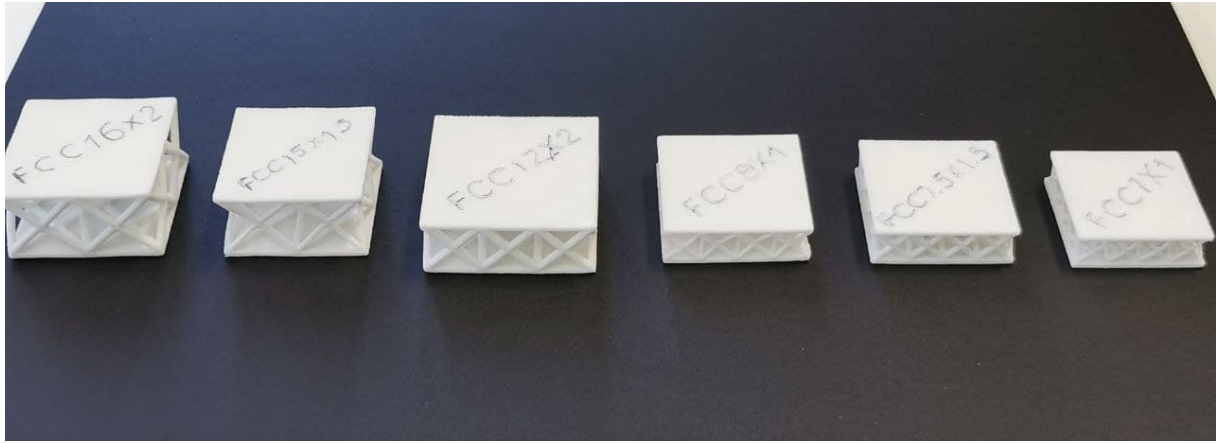


Figure 5.4: Printed specimens with FCC configuration.

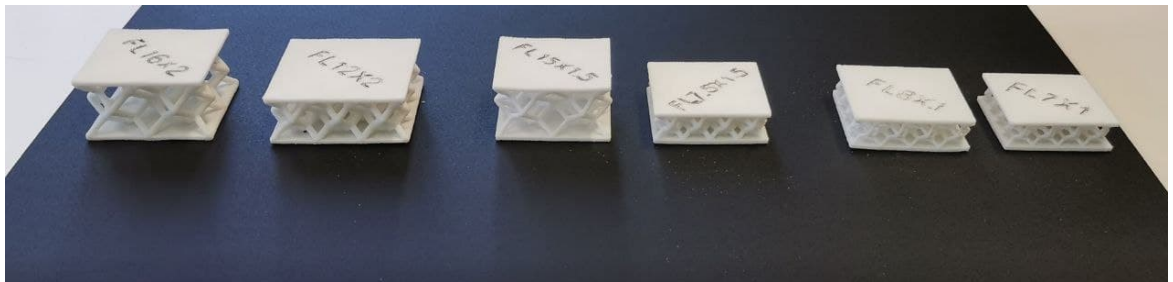


Figure 5.5: Printed specimens with Fluorite configuration.

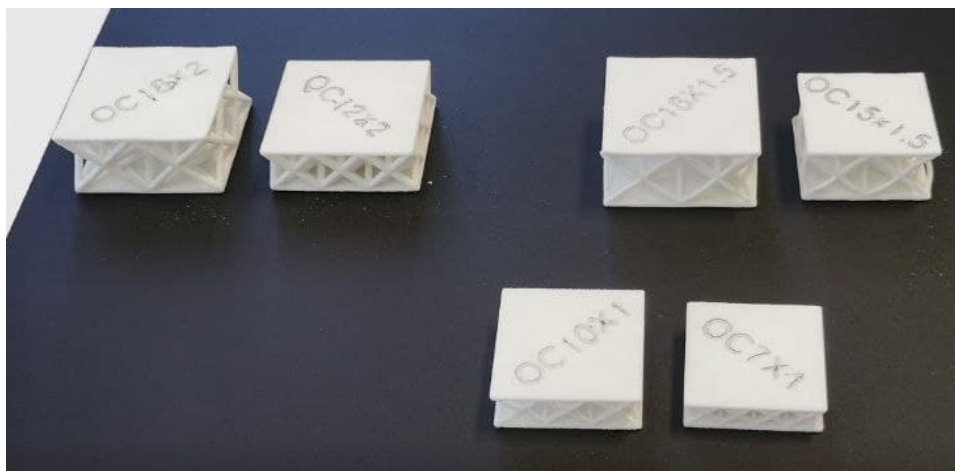


Figure 5.6: Printed specimens with Octet configuration.

6 Conclusion

This study proposes a method to design a custom-made insole to reduce plantar stress and prevent the risk of foot ulceration and recurrence, particularly for those patients with diabetic foot syndrome with neuropathy. Modern CAD technology allows the design of customized insoles starting from the foot geometry in combination with the pressure map. In this study, lattice structures are used to relieve plantar stress and lighten the insole. Six topologies, Body Centered Cubic (BCC), Simple Cubic, Diamond, Face Centered Cubic(FCC), Octet, Fluorite are used to generate the lattice structure. Several specimens are constructed with the lattice structures of the different topologies to study the behavior of the unit cells. The material selected for design the insole and the specimens is the Thermoplastic polyurethane TPU and its material properties are employed in the modeling work. The mechanical responses are investigated with the finite element analysis. The specimens are build, designed and simulated using the nTopology software. The mechanical response proves that the lattice structure with different topology can influence the property of the specimen. Therefore, it is possible to control the property of the insole with different lattice structures.

The Octet topology is found to be the most rigid of all designs and has the best and most uniform stress distribution. The Simple cubic, BCC and Diamond have high deformation and good energy absorption but due to the elevated internal stress, these structures are discarded. On the other hand, Fluorite and FCC had properties similar to those of the Octet, with a good rigidity and stress distributions. Therefore, the Octet, FCC and Fluorite, are considered to design the insoles and some specimens made with these cells are printed with the SLS technique to evaluate the properties of the specimens made, the quality of the print and the material used. Even the insole is modeled and constructed, changing the distribution of material, with the same software.

NTopology has demonstrated good creation and processing skills with lattice structures and an interesting method to directly drive and control advanced geometry by using biometric measurements or experimental data. In fact, even for the insoles made, it is possible to observe a good ability to create areas with different properties, (material distribution) by using the loading maps. A limitation in the design process used is that by filling the insole with a periodic lattice structure, the cells will be trim at the edges (in the points where the lattice structure intersects the model of the insole) thus forgiving the mechanical properties that characterized the single cell.

For what concern the specimens made with the SLS process, they have good component qualities even in the thinnest ones and high detail accuracy.

Therefore, also for the eventual manufacturing of the insole can be considered the SLS and an object with high precision is expected. This technique has proven to be a good low-cost printing process (among the cheapest), for fine quality objects, but it is also possible to perform an evaluation with other methods to verify printability, such as FDM.

Future studies will be able to carry out the experimental verification of the specimens printed and compare these results with those collected from the numerical analysis. Simulating and replacing the contact mechanism between foot and insole with that of the stresses acting on the specimens can be a bit reductive, a limitation of the study, because it doesn't take into account various factors such as the fatigue behavior of the created structures, the shape of the plantar that is not linear and homogeneous but changes by cutting the various cells and modifying their properties, or the plantar stresses and their variation during the dynamic phase of the gait cycle in which it is subjected.

The fatigue behavior is an important and fundamental aspect to consider as it gives information on the durability of the insole, but difficult to study with numerical analysis.

On the other hand, it can also be studied in depth with experimental analyses using the printed specimens. As for the plantar stresses that act during the different phases of the footstep of a subject, these should be collected in the laboratory through the maps and then analyzed to create a customized insole, starting from the scan of a subject's foot.

Future studies will use the results of this analysis and use the selected cells to create a finite element model of the customized insole starting from a foot scan. The insole will be made using the lattice structure, beginning the profile of the three-dimensional FE shape of the foot and with the creation of a model to study the contact mechanics of the interface between the foot and the insole.

Other cells can also be considered to make the insole, such as TPMS which have been shown to have good energy absorbing properties. An experimental test can be carried out on the 3D printing insole to validate the model and verify the effectiveness of the insole in redistributing pressure compared to a flat insole.

7 Bibliography

- [1] Nalini Singh , David G Armstrong, Benjamin A Lipsky. Preventing foot ulcers in patients with diabetes. 2005 Jan 12;293(2):217-28.
- [2] Richard Collings, Jennifer Freeman, Jos M. Latour,Joanne Paton. Footwear and insole design features for offloading the diabetic at risk foot – A systematic review and meta-analyses, 11 April 2020.
- [3] Armstrong DG, Boulton AJM, Bus SA. Diabetic foot ulcers and their recurrence. *N Engl J Med.*; 376(24): 2367- 2375; 2017
- [4] Waaijman R, de Haart M, Arts ML, et al. Risk factors for plantar foot ulcer recurrence in neuropathic diabetic patients. *Diabetes Care.* 37(6): 1697- 1705; 2014.
- [5] Malindu Eranga Fernando ,Robert George Crowther. Plantar Pressure in Diabetic Peripheral Neuropathy Patients with Active Foot Ulceration, Previous Ulceration and No History of Ulceration: A Meta-Analysis of Observational Studies; Kunwarjit Singh Sangla,Petra Buttner,Jonathan Golledge; 2014.
- [6] Roelof Waaijman, Mirjam de Haart, Mark L.J. Arts, Daniel Wever. Risk Factors for Plantar Foot Ulcer Recurrence in Neuropathic Diabetic Patients; *Diabetes Care* 2014;37:1697–1705.
- [7] H J Murray , M J Young, S Hollis, A J Boulton. The association between callus formation, high pressures and neuropathy in diabetic foot ulceration *Diabet Med.* 1996 Nov;13(11):979-82.
- [8] Metin Yavuz, Ahmet Erdemir, , Georgeanne Botek, , Gordon B. Peak Plantar Pressure and Shear Locations; *Diabetes Care* 2007 Oct; 30(10): 2643-2645.
- [9] Veves A, Murray HJ, Young MJ, Boulton AJ. The risk of foot ulceration in diabetic patients with high foot pressure: a prospective study. *Diabetologia* 35:660–663, 1992.
- [10]Metin Yavuz, Ali Ersen, Jessica Hartos, Brandy Schwarz. Plantar Shear Stress in Individuals With a History of Diabetic Foot Ulcer: An Emerging Predictive Marker for Foot Ulceration; *Diabetes Care* 2017 Feb; 40(2): e14-e15.

- [11] Lord M, Hosein R. A study of in-shoe plantar shear in patients with diabetic neuropathy. *Clin Biomech (Bristol, Avon)* 15:278–283, 2000.
- [12] Perry JE, Hall JO, Davis BL. Simultaneous measurement of plantar pressure and shear forces in diabetic patients. *Gait Posture* 15:101–107, 2002.
- [13] Yavuz M, Master H, Garrett A, Lavery LA. Peak plantar shear and pressure and foot ulcer locations: a call to revisit ulceration pathomechanics. *Diabetes Care*;38: e184–e185; 2015.
- [14] Abdul Hadi Abdul Razak, Aladin Zayegh, Rezaul K. Begg, Yufridin Wahab. Foot Plantar Pressure Measurement System: A Review. *Sensors (Basel)*. 2012; 12(7): 9884–9912.
- [15] Gefen A. Pressure-sensing devices for assessment of soft tissue loading under bony prominences: Technological concepts and clinical utilization. *Wounds*. 2007;19:350–362.
- [16] MacWilliams B.A., Armstrong P.F. Clinical Applications of Plantar Pressure Measurement in Pediatric Orthopedics. *Proceeding of Pediatric Gait, 2000. A New Millennium in Clinical Care and Motion Analysis Technology*; Chicago, IL, USA. 22 July 2000; pp. 143–150.
- [17] Margo N Orlin, Thomas G McPoil. Plantar Pressure Assessment. *Physical Therapy, Volume 80, Issue 4, 1 April 2000, Pages 399–409*.
- [18] Matthew L. Maciejewski, Gayle E. Reiber, Douglas Smith. Effectiveness of Diabetic Therapeutic Footwear in Preventing Reulceration. August 2004 *Diabetes Care* 27(7):1774-82.
- [19] Musab Ibrahim , Rana El Hilaly , Mona Taher , Ahmed Morsy. A pilot study to assess the effectiveness of orthotic insoles on the reduction of plantar soft tissue strain. *Clinical Biomechanics* volume 28, issue 1, p68-72, 2013.
- [20] Miguel Davia-Aracil, Juan José Hinojo-Pérez, Antonio Jimeno-Morenilla. 3D Printing of Functional Anatomical Insoles. *Computers in Industry* Volume 95, February 2018, Pages 38-53.
- [21] Tammy M. Owings, Deng Julie L. Woerner, Bs Jason D. Frampton. Custom Therapeutic Insoles Based on Both Foot Shape and Plantar Pressure Measurement Provide Enhanced Pressure Relief. *Diabetes Care* 31:839–844, 2008.

- [22] Mandolini, Marco; Brunzini, Agnese; Manieri, Steve; Germani, Michele. Foot Plantar Pressure Offloading: How To Select The Right Material For A Custom Made Insole. 21st international conference on engineering design, iced17, 2017.
- [23] M. Mandolini, M., Germani, R. Raffaelli . Finite Element Method to support the materials selection phase during the insole design process. Università Politecnica delle Marche, Department of Industrial Engineering.
- [24] Richard ,Jennifer Freeman, Jos M. Latour, Joanne Paton. Footwear and insole design features for offloading the diabetic at risk foot –A systematic review and meta-analyses. *Endocrinol Diabetes Metab.* 4(1): e00132. 2021.
- [25] Owings TM, Woerner JL, Frampton JD, Cavanagh PR, Botek G. Custom therapeutic insoles based on both foot shape and plantar pressure measurement provide enhanced pressure relief. *Diabetes Care.*31(5):839-844;2008.
- [26] Mueller MJ, Lott DJ, Hastings MK, Commean PK, Smith KE, Pilgram TK. Efficacy and mechanism of orthotic devices to unload metatarsal heads in people with diabetes and a history of plantar ulcers. *Phys Ther.*86(6):833-842; 2006.
- [27] Lawrence A Lavery, Dan R Lanctot, George Constantinides. Wear and Biomechanical Characteristics of a Novel Shear-Reducing Insole with Implications for High-Risk Persons with Diabetes. *Diabetes Technology & Therapeutics* 7(4):638-46; 2005.
- [28] Marinelli, Paola; Mandolini, Marco; Germani, Michele. A Knowledge-Based Design Process For Custom Made Insoles. International conference on engineering design, iced 2015.
- [29] Chung-Neng Huang, Ming-Yih Lee and Chong-Ching Chang, (2011). Computer-aided design and manufacturing of customized insoles. *IEEE computer graphics and applications*, Vol.31, No.2, pp.74-79.
- [30] L. Fangyu, L. Yefei, W. Meiqiong, W. Jianfeng. Research on Computer Aided Design of Customized Insoles, *Computer-Aided Industrial Design & Conceptual Design*, 1430-1433, 2009.

- [31] Jason Tak-Man Cheung, MPhil. A 3-dimensional finite element model of the human foot and ankle for insole design. Volume 86, Issue 2, P353-358, February 01, 2005.
- [32] ParoCountour®-System,
<https://paromed.de/medien/medienpool/paroContour-System-4S-EN2.pdf>,
 Paromed.
- [33] IcadPAN INESCOPE, <https://www.inescop.es/en/services/software-for-footwear>, INESCOP
- [34] C.E. Dombroski, A. Froats and M.E.R. Balsdon. The use of a low cost 3D scanning and printing tool in the manufacture of custom-made foot orthoses: a preliminary study. BMC Res. Notes, 7 (2014), pp. 443-447
- [35] Ulla Hellstrand Tang, Roland Zügner, Vera Lisovskaja. Comparison of plantar pressure in three types of insole given to patients with diabetes at risk of developing foot ulcers - A two-year, randomized trial. J Clin Transl Endocrinol. 2014 Jul 24;1(4):121-132.
- [36] Lo, W T et al. Effects of custom-made textile insoles on plantar pressure distribution and lower limb EMG activity during turning. Journal of foot and ankle research vol. 9 22. 13 Jul. 2016, doi:10.1186/s13047-016-0154-5.
- [37] Phil Reeves, Christopher John Tuck, Richard J.M.Hague. Additive Manufacturing for Mass Customization. In book: Mass Customization.
- [38] Miguel Davia-Aracil, Juan José Hinojo-Pérez, Antonio Jimeno-Morenilla, Higinio Mora-Mora. **3D Printing of Functional Anatomical Insoles**. Spanish Footwear Technology Institute (INESCOP), Polígono Campo Alto, Spain
- [39] Hyunwoong KoSeungKi, MoonSeung MoonJihong, HwangJihong Hwang. Design for additive manufacturing in customized products. International Journal of Precision Engineering and Manufacturing 16(11):2369-2375 2005
- [40] Additive Manufacturing Technique. Comprehensive Materials Processing, 2014
- [41] Guide to Selective Laser Sintering (SLS) 3D Printing.
<https://formlabs.com/blog/what-is-selective-laser-sintering/>
- [42] An evaluation of personalized insoles developed using additive manufacturing

- [43] Salles, A.S., & Gyi, D.E. (2012). Delivering personalised insoles to the high street using additive manufacturing. *International Journal of Computer Integrated Manufacturing*
- [44] Guoying Dong, Daniel Tessier, Yaoyao Fiona, ZhaoYaoyao, Fiona Zhao. Design of Shoe Soles Using Lattice Structures Fabricated by Additive Manufacturing. *Proceedings of the Design Society International Conference on Engineering Design* 1(1):719-728
- [45] Lei Tanga , Ling Wanga , Wannan Baoa , Siyao Zhua , Dichen Lia,* , Ningxin'er Zhaoa , Chaozong Liub Functional gradient structural design of customized diabetic insoles. *Journal of the Mechanical Behavior of Biomedical Materials* Volume 94, June 2019, Pages 279-287
- [46] Nouman M, Dissaneewate T, Chong DYR, Chatpun S. Effects of Custom-Made Insole Materials on Frictional Stress and Contact Pressure in Diabetic Foot with Neuropathy: Results from a Finite Element Analysis. *Applied Sciences*. 2021; 11(8):3412.
- [47] Lefan Wang, Member, Dominic Jones, Graham. A Review of Wearable Sensor Systems to Monitor Plantar Loading in the Assessment of Diabetic Foot Ulcers. *IEEE Transactions on Biomedical Engineering*, 67 (7). pp. 1989-2004. ISSN 0018-9294
- [48]Wenjin Tao; Ming C. Leu :Design of lattice structure for additive manufacturing
- [49] Pan, C.; Han, Y.; Lu, J. Design and Optimization of Lattice Structures: A Review. *Appl. Sci.* 2020, 10, 6374.
- [50] Tobias Maconachie, Martin Leary, Bill Lozanovski, Xuezhe Zhang, Ma Qian, SLM lattice structures: Properties, performance, applications and challenges, *Materials & Design*, Volume 183, 2019,
- [51]Mark Helou & Sami Kara (2018) Design, analysis and manufacturing of lattice structures: an overview, *International Journal of Computer Integrated Manufacturing*, 31:3, 243-261.
- [52] Chen, Y. 3D Texture Mapping for Rapid Manufacturing. *Comput. Aided Des. Appl.* 2007, 4, 761-771.

8 Appendix

Table 8.1: Results of the numerical analysis with the samples: first part.

UNIT CELL TYPE	CELL DIMENSION (mm)	STRUCT SIZE (mm)	Printed	DENSITY	NORMAL PRESSURE (KPa)	SHEAR FORCE (N)	HORIZONTAL DISPLACEMENT (mm)	VERTICAL DISPLACEMENT (mm)	HORIZONTAL DISPLACEMENT / VERTICAL DISPLACEMENT
FCC	15	1,5	Yes	19%	150	61	2,37	3,27	0,72
FCC	16	2	Yes	21%	225	90	2,17	3,10	0,70
FCC	16	2	Yes	21%	300	120	2,90	4,13	0,70
FCC	16	2	Yes	21%	150	61	1,43	2,05	0,70
FCC	12	2	Yes	29%	150	61	0,47	1,10	0,43
FCC	8	1	Yes	28%	150	61	0,68	0,75	0,91
FCC	7	1	Yes	34%	150	61	0,55	0,45	1,22
FCC	7,5	1,5	Yes	41%	150	61	0,27	0,22	1,23
FLUORITE	15	1,5	Yes	20%	150	61	5,56	3,40	1,64
FLUORITE	16	2	Yes	23%	150	61	2,70	1,96	1,38
FLUORITE	16	2	Yes	23%	300	120	5,32	3,90	1,36
FLUORITE	16	2	Yes	23%	225	90	3,98	2,90	1,37
FLUORITE	8	1	Yes	31%	150	61	0,77	0,53	1,45
FLUORITE	7	1	Yes	37%	150	61	0,51	0,29	1,76
FLUORITE	12	2	Yes	33%	150	61	0,44	0,41	1,07
FLUORITE	7,5	1,5	Yes	46%	150	61	0,18	0,13	1,38
OCTET	18	1,5	Yes	19%	150	61	1,71	2,37	0,72
OCTET	15	1,5	Yes	24%	300	120	2,74	2,67	1,03
OCTET	15	1,5	Yes	24%	225	90	2,11	1,97	1,07
OCTET	15	1,5	Yes	24%	150	61	1,39	1,31	1,06
OCTET	10	1	Yes	28%	150	61	0,83	0,79	1,05
OCTET	18	2	Yes	23%	150	61	0,93	1,24	0,75
OCTET	7	1	Yes	41%	150	61	0,26	0,20	1,30
OCTET	12	2	Yes	39%	150	61	0,22	0,27	0,81
OCTET	9	1,5	Yes	44%	150	61	0,28	0,20	1,40
OCTET	4	1,5	No	89%	150	61	0,23	0,11	2,09
FLUORITE	4	1,5	No	78%	150	61	0,29	0,13	2,23
FCC	4	1,5	No	67%	150	61	0,51	0,26	1,96
OCTET	4	1	No	60%	150	61	0,50	0,30	1,67
FLUORITE	4	1	No	53%	150	61	0,62	0,35	1,77
DIAMOND	4	1,5	No	57%	150	61	0,60	0,35	1,71
BCC	4	1,5	No	57%	150	61	0,68	0,46	1,48
SIMPLE CUBIC	4	1,5	No	40%	150	61	3,03	0,75	4,04
FCC	4	1	No	43%	150	61	1,24	0,76	1,63

DIAMOND	4	1	No	37%	150	61	1,63	1,09	1,50
SIMPLE CUBIC	4	1	No	27%	150	61	10,83	1,60	6,77
BCC	4	1	No	37%	150	61	1,80	1,54	1,17
FCC	5	1,5	No	54%	150	61	0,58	0,38	1,53
DIAMOND	5	1,5	No	46%	150	61	0,70	0,52	1,35
OCTET	5	1	No	49%	150	61	0,62	0,49	1,27
FLUORITE	5	1	No	43%	150	61	0,90	0,66	1,36
BCC	5	1,5	No	46%	150	61	0,77	0,68	1,13
SIMPLE CUBIC	5	1,5	No	35%	150	61	4,89	0,97	5,04
FCC	5	1	No	36%	150	0	1,47	1,15	1,28
DIAMOND	5	1	No	32%	150	61	2,22	1,69	1,31
SIMPLE CUBIC	5	1	No	26%	150	61	21,15	2,21	9,57
BCC	5	1	No	32%	150	61	2,03	2,16	0,94
OCTET	6	1,7	No	73%	150	61	0,37	0,24	1,54
FLUORITE	6	1,7	No	63%	150	61	0,50	0,31	1,61
OCTET	6	1,5	No	65%	150	61	0,50	0,35	1,43
FLUORITE	6	1,5	No	56%	150	61	0,70	0,46	1,52
FCC	6	1,7	No	54%	150	61	0,89	0,65	1,37
DIAMOND	6	1,7	No	46%	150	61	1,11	0,87	1,28
FCC	6	1,5	No	48%	150	61	1,18	0,91	1,30
DIAMOND	6	1,5	No	41%	150	61	1,72	1,28	1,34
SIMPLE CUBIC	6	1,7	No	37%	150	61	8,20	1,49	5,50
BCC	6	1,7	No	46%	150	61	1,22	1,31	0,93
SIMPLE CUBIC	6	1,5	No	33%	150	61	11,98	1,91	6,27
BCC	6	1,5	No	41%	150	61	1,81	1,88	0,96
OCTET	7	2,2	No	78%	150	61	0,46	0,24	1,92
FLUORITE	7	2,2	No	67%	150	61	0,63	0,3	2,10
OCTET	7	1,8	No	65%	150	61	0,74	0,42	1,76
FLUORITE	7	1,8	No	57%	150	61	1,08	0,57	1,89
FCC	7	2,2	No	60%	150	61	1,03	0,56	1,84
DIAMOND	7	2,2	No	51%	150	61	1,57	0,91	1,73
FCC	7	1,8	No	50%	150	61	1,65	1	1,65
SIMPLE CUBIC	7	2,2	No	41%	150	61	6,75	1,36	4,96
BCC	7	2,2	No	51%	150	61	1,72	1,18	1,46
DIAMOND	7	1,8	No	43%	150	61	2,8	1,71	1,64
SIMPLE CUBIC	7	1,8	No	36%	150	61	14,58	2,07	7,04
BCC	7	1,8	No	43%	150	61	3,03	2,37	1,28
OCTET	8	2,5	No	76%	150	61	0,38	0,26	1,46
FLUORITE	8	2,5	No	65%	150	61	0,51	0,32	1,59
FCC	8	2,5	No	57%	150	61	0,87	0,62	1,40
DIAMOND	8	2,5	No	48%	150	61	1,28	0,99	1,29
SIMPLE CUBIC	8	2,5	No	38%	150	61	6,16	1,52	4,05
BCC	8	2,5	No	49%	150	61	1,37	1,23	1,11

Table 8.2: Results of the numerical analysis with the samples: second part.

UNIT CELL TYPE	CELL DIMENSION (mm)	STRUCT SIZE (mm)	HORIZONTAL DISPLACEMENT * DENSITY	VERTICAL DISPLACEMENT * DENSITY	VERTICAL STIFFNESS [MPa]	HORIZONTAL STIFFNESS [Mpa]	VON MISES STRESS (Pa)	VON MISES STRESS * DENSITY
FCC	15	1,5	0,46	0,63	0,78	0,83	7,03E+07	1,35E+07
FCC	16	2	0,45	0,65	1,31	1,22	6,77E+07	1,41E+07
FCC	16	2	0,60	0,86	1,31	1,22	9,03E+07	1,88E+07
FCC	16	2	0,30	0,43	1,32	1,25	4,53E+07	9,43E+06
FCC	12	2	0,14	0,32	1,91	3,42	4,44E+07	1,28E+07
FCC	8	1	0,19	0,21	2,00	2,72	3,61E+07	1,01E+07
FCC	7	1	0,19	0,15	3,00	3,82	2,94E+07	9,91E+06
FCC	7,5	1,5	0,11	0,09	6,48	7,29	1,30E+07	5,33E+06
FLUORITE	15	1,5	1,14	0,70	0,75	0,35	2,09E+08	4,27E+07
FLUORITE	16	2	0,61	0,44	1,38	0,66	6,94E+07	1,56E+07
FLUORITE	16	2	1,20	0,88	1,38	0,66	1,38E+08	3,11E+07
FLUORITE	16	2	0,90	0,65	1,40	0,67	1,04E+08	2,33E+07
FLUORITE	8	1	0,24	0,16	2,83	2,40	4,92E+07	1,51E+07
FLUORITE	7	1	0,19	0,11	4,66	4,12	4,15E+07	1,53E+07
FLUORITE	12	2	0,14	0,13	5,12	3,65	3,10E+07	1,01E+07
FLUORITE	7,5	1,5	0,08	0,06	10,96	10,93	1,93E+07	8,96E+06
OCTET	18	1,5	0,32	0,44	1,27	0,96	4,95E+07	9,28E+06
OCTET	15	1,5	0,65	0,63	1,91	1,41	4,36E+07	1,03E+07
OCTET	15	1,5	0,50	0,47	1,94	1,38	3,22E+07	7,63E+06
OCTET	15	1,5	0,33	0,31	1,95	1,42	2,19E+07	5,20E+06
OCTET	10	1	0,23	0,22	2,28	2,37	2,98E+07	8,26E+06
OCTET	18	2	0,22	0,29	2,42	1,73	2,47E+07	5,74E+06
OCTET	7	1	0,11	0,08	6,75	8,09	1,40E+07	5,73E+06
OCTET	12	2	0,09	0,10	7,78	7,30	9,49E+06	3,68E+06
OCTET	9	1,5	0,12	0,09	8,25	7,78	8,74E+06	3,82E+06
OCTET	4	1,5	0,21	0,10	19,09	9,15	2,78E+06	2,49E+06
FLUORITE	4	1,5	0,23	0,10	16,15	7,25	3,16E+06	2,45E+06
FCC	4	1,5	0,34	0,17	8,08	4,12	4,80E+06	3,22E+06
OCTET	4	1	0,30	0,18	7,00	4,21	7,83E+06	4,73E+06
FLUORITE	4	1	0,33	0,19	6,00	3,39	8,06E+06	4,26E+06
DIAMOND	4	1,5	0,34	0,20	6,00	3,51	5,64E+06	3,21E+06
BCC	4	1,5	0,39	0,26	4,57	3,09	1,16E+07	6,58E+06
SIMPLE CUBIC	4	1,5	1,22	0,30	2,80	0,69	1,18E+07	4,75E+06
FCC	4	1	0,53	0,32	2,76	1,70	1,15E+07	4,92E+06
DIAMOND	4	1	0,60	0,40	1,93	1,29	1,89E+07	6,94E+06
SIMPLE CUBIC	4	1	2,97	0,44	1,31	0,19	4,45E+07	1,22E+07
BCC	4	1	0,66	0,56	1,36	1,17	4,01E+07	1,47E+07
FCC	5	1,5	0,32	0,21	4,74	3,39	5,57E+06	3,04E+06

DIAMOND	5	1,5	0,32	0,24	3,46	2,81	7,74E+06	3,58E+06
OCTET	5	1	0,31	0,24	3,67	3,17	7,90E+06	3,90E+06
FLUORITE	5	1	0,39	0,28	2,73	2,19	1,54E+07	6,62E+06
BCC	5	1,5	0,36	0,31	2,65	2,56	1,63E+07	7,54E+06
SIMPLE CUBIC	5	1,5	1,70	0,34	1,86	0,40	2,16E+07	7,49E+06
FCC	5	1	0,53	0,42	1,57	0,00	1,54E+07	5,60E+06
DIAMOND	5	1	0,71	0,54	1,07	0,89	3,06E+07	9,75E+06
SIMPLE CUBIC	5	1	5,46	0,57	0,81	0,09	8,09E+07	2,09E+07
BCC	5	1	0,65	0,69	0,83	0,97	2,64E+07	8,42E+06
OCTET	6	1,7	0,27	0,18	9,38	5,32	3,41E+06	2,49E+06
FLUORITE	6	1,7	0,31	0,19	7,26	3,94	5,36E+06	3,37E+06
OCTET	6	1,5	0,32	0,23	6,43	3,94	4,61E+06	2,98E+06
FLUORITE	6	1,5	0,39	0,26	4,89	2,81	9,68E+06	5,40E+06
FCC	6	1,7	0,48	0,35	3,46	2,21	6,69E+06	3,63E+06
DIAMOND	6	1,7	0,51	0,40	2,59	1,77	1,02E+07	4,70E+06
FCC	6	1,5	0,57	0,44	2,47	1,67	9,64E+06	4,63E+06
DIAMOND	6	1,5	0,71	0,53	1,76	1,14	1,29E+07	5,33E+06
SIMPLE CUBIC	6	1,7	3,00	0,55	1,51	0,24	2,61E+07	9,56E+06
BCC	6	1,7	0,56	0,61	1,72	1,61	1,57E+07	7,27E+06
SIMPLE CUBIC	6	1,5	4,01	0,64	1,18	0,16	3,15E+07	1,05E+07
BCC	6	1,5	0,75	0,78	1,20	1,09	1,69E+07	7,01E+06
OCTET	7	2,2	0,36	0,19	11,25	4,42	2,98E+06	2,34E+06
FLUORITE	7	2,2	0,42	0,20	9,00	3,23	4,07E+06	2,74E+06
OCTET	7	1,8	0,48	0,27	6,43	2,75	4,97E+06	3,25E+06
FLUORITE	7	1,8	0,61	0,32	4,74	1,88	1,33E+07	7,50E+06
FCC	7	2,2	0,62	0,34	4,82	1,97	6,34E+06	3,81E+06
DIAMOND	7	2,2	0,80	0,46	2,97	1,30	8,22E+06	4,18E+06
FCC	7	1,8	0,82	0,50	2,70	1,23	9,84E+06	4,92E+06
SIMPLE CUBIC	7	2,2	2,79	0,56	1,99	0,30	2,06E+07	8,53E+06
BCC	7	2,2	0,87	0,60	2,29	1,18	1,42E+07	7,19E+06
DIAMOND	7	1,8	1,20	0,74	1,58	0,73	1,40E+07	6,01E+06
SIMPLE CUBIC	7	1,8	5,25	0,75	1,30	0,14	3,14E+07	1,13E+07
BCC	7	1,8	1,30	1,02	1,14	0,67	2,26E+07	9,70E+06
OCTET	8	2,5	0,29	0,20	11,54	4,72	3,06E+06	2,34E+06
FLUORITE	8	2,5	0,33	0,21	9,38	3,52	4,28E+06	2,80E+06
FCC	8	2,5	0,50	0,35	4,84	2,06	6,29E+06	3,60E+06
DIAMOND	8	2,5	0,62	0,48	3,03	1,40	7,42E+06	3,60E+06
SIMPLE CUBIC	8	2,5	2,34	0,58	1,97	0,29	1,83E+07	6,96E+06
BCC	8	2,5	0,67	0,60	2,44	1,31	1,98E+07	9,63E+06